Molecular dynamics in the process of autophagosome formation in yeast

Kuninori Suzuki

Department of Molecular Biomechanics
Graduate Program in School of Life Science
The Graduate University for Advanced Studies

Acknowledgements

I wish to express my deepest appreciation to Prof. Yoshinori Ohsumi for constant supervision and encouragement for gaining my motivation to struggle with the complex phenomena autophagy. I wish to express my appreciation to other members of Ohsumi laboratory: Drs. Tamotsu Yoshimori, Yoshiaki Kamada, Takeshi Noda and Misuzu Baba, Ms. Yukiko Kabeya, Drs. Noboru Mizushima, Takahiro Shintani, Naotada Ishihara, Takayuki Sekito, Akio Kihara, Kohki Yoshimoto, Takayoshi Kirisako, Mr. Yoshinobu Ichimura, Atsuki Nara, Hideki Hanaoka, Yoshinori Kobayashi, Ms. Shisako Shoji, Akiko Kuma, Maho Hamasaki, Mr. Jun Onodera, Ms. Satsuki Okamoto, Mio Ito and Kumi Tsukeshiba. I wish to express my gratitude to Drs. Daniel J. Klionsky, Kazuma Tanaka and Mark S. Longtine for plasmids, Dr. Scott D. Emr for a strain, and Dr. Hiroshi Abe for antiserum. I would also like to thank Mr. Takaji Nemoto, Drs. Tokuko Haraguchi and Yasushi Hiraoka for their technical advice on fluorescence microscopy.

Contents

List of Figures

List of Tables

Abbreviations

3MA	3-metyladenine
ALP	alkaline phosphatase
API	aminopeptidase I
BSA	bovine serum albumin
CA	casamino acid
CFP	cyan fluorescent protein
CPY	carboxypeptidase Y
Cvt	cytosol-to-vacuole targeting
DMSO	dimethylsulfoxide
EDTA	ethylenediamine tetraacetic acid
EGTA	ethylene glycol bis(β-aminoethylether)-tetraacetic acid
ER	endoplasmic reticulum
FBPase	fructose-1,6-bisphosphatase
HA	hemagglutinin
GFP	green fluorescent protein
mAPI	mature aminopeptidase I
OD	optical density
ORF	open reading frame
PAGE	polyacrylamide gel electrophoresis
PBS	phosphate-buffered saline
PCR	polymerase chain reaction
PE	phosphatidylethanolamine
PI3-kinase	phosphatidylinositol-3 kinase
PI3P	phosphatidylinositol 3-phosphate
PMSF	phenylmethylsulfoyl fluoride
proAPI	precursor form of aminopeptidase I
RER	rough endoplasmic reticulum
SD	synthetic dextrose medium
SDS	sodium dodecyl sulfate
SNARE	soluble N-ethylmaleimide-sensitive fusion protein attachment protein receptor
YFP	yellow fluorescent protein

Summary

Macroautophagy is a bulk degradation process induced by starvation in eukaryotic cells. In yeast, *Saccharomyces cerevisiae*, at least 15 Apg proteins are essential for the formation of autophagosomes. Recently, several key reactions mediated by Apg proteins have been described: two ubiquitin-like conjugation systems, a phosphatidylinositol 3-kinase (PI3-kinase) system and a protein kinase system. Two ubiquitin-like systems consist of Apg12 system and Aut7/Apg8 system. Apg12p, Apg7p, Apg10p, Apg5p and Apg16p are involved in Apg12 system. This system finally produces a stable complex, namely the Apg12p-Apg5p-Apg16p complex. In Aut7 system, phosphatidylethanolamine-conjugated Aut7p (Aut7p-PE), which is required for the progression of autophagy, is generated by the sequential reactions of Aut2p/Apg4p, Apg7p and Aut1p/Apg3p to Aut7p. Vps30p/Apg6p and Apg14p form a specific PI3-kinase complex essential for autophagy. The protein kinase complex is composed of Apg1p, Apg13p and Apg17p. The kinase activity of Apg1p is enhanced by induction of autophagy. Despite of such detailed molecular analyses, the overall network between these reactions still remains to be elucidated.

Electron microscopic study showed that Aut7p is localized on the membranes of autophagosomes in the course of formation, and finally in the lumen of autophagosomes. Green fluorescent protein (GFP)-fused Aut7p was constructed and its dynamics was examined by fluorescence microscopy. GFP-Aut7p labeled autophagosomes, autophagic bodies and a novel structure which I designated as the pre-autophagosomal structure. Further analyses demonstrated that this pre-autophagosomal structure, containing at least five Apg proteins, i. e. Apg1p, Apg2p, Apg5p, Aut7p and Apg16p, is localized in the vicinity of the vacuole and directly involved in autophagosome formation. Analysis of *apg* mutants revealed that the formation of both Aut7p-PE and the Apg12p-Apg5p conjugate is essential for the localization of Aut7p to the pre-autophagosomal structure. Vps30p and Apg14p, components of an autophagy-specific PI3-kinase complex, Apg9p and Apg16p are all required for the localization of Apg5p and Aut7p to the structure. The Apg1p protein kinase complex functions in the late stage of autophagosome formation on the pre-autophagosomal structure. The pre-autophagosomal structure, which is organized by concerted interactions of two conjugation systems and the PI3-kinase system, plays a pivotal role in autophagosome formation.

Aminopeptidase I (API) is a vacuolar hydrolase, which is selectively delivered via autophagosomes under starvation conditions and becomes mature form after processing by

vacuolar proteases. Electron microscopic study demonstrated that the proform of API forms the cytosol-to-vacuole targeting (Cvt) complex, which is enwrapped by autophagosome and delivered to the vacuole. I constructed a strain expressing API-GFP and investigated the dynamics of cargo delivery by autophagosome. Fluorescence microscopy showed that API-GFP is concentrated on a dot close to the vacuole. This dot, which corresponds to the Cvt complex, mostly appears very close to the pre-autophagosomal structure. Interestingly, formation of the Cvt complex is not impaired in the absence of any Apg protein examined or Cvt19p, a receptor for the Cvt pathway. The time-lapse observation using *apg1*^{ts} cells clarified that the Cvt complex stays outside the vacuole at the non-permissive temperature and is transported to the vacuole after shifting to the permissive temperature. The whole Cvt complex is delivered to the vacuole by one step, indicating the complex is engulfed into one autophagosome. The complex, which entered the vacuole, is immediately disintegrated and diffused throughout the vacuole in one minute. API-GFP enables me to analyze the localization of Cvt complexes and the dynamics of cargo delivery mediated by autophagosome.

In this study, I discovered and described the pre-autophagosomal structure involved in generating autophagosomes. Several Apg proteins are converged upon the structure as a consequence of interaction of Apg proteins. Moreover, I successfully visualized the process of a cargo transport to the vacuole with API-GFP. API forms a Cvt complex on the pre-autophagosomal structure. This complex is enclosed into autophagosome and finally delivered to the vacuole. Here, I described the overall image of autophagosome formation and cargo delivery during autophagy by GFP-Aut7p and API-GFP as markers of autophagosome and the pre-autophagosomal structure, and a cargo, respectively.

Introduction

Protein degradation in eukaryotes

Molecular biological studies on the topic of cellular regulation have focused on protein synthesis and the control of gene expression. However, it is clear that every cellular activity is maintained by a delicate balance between synthesis and breakdown of individual proteins. Recently, protein degradation has become a field of intense study in cell biology because it has been revealed to play critical roles in many aspects of cellular regulation.

Most of the selective protein degradation is believed to occur in the cytosol through the action of the ubiquitin/proteasome system (Hilt and Wolf, 1995). In contrast, major bulk protein degradation takes place in the lytic compartment, the lysosome/vacuole. Nonspecific protein turnover has essential roles under nutrient stress or for differentiation of eukaryotic cells. Until now, the molecular details of protein degradation in the lytic compartment remained unknown due to the lack of a sensitive assay system to monitor the disappearance of proteins. In addition, the dynamic features of the lysosomal/vacuolar membrane system have complicated investigation into this complex cellular process.

Ubiquitin system: selective protein degradation

The ubiquitin system carries out the selective degradation of many short-lived cytosolic proteins in eukaryotes (Hochstrasser, 1996; Varshavsky, 1997; Ciechanover, 1998; Hershko and Ciechanover, 1998). Proteins ligated ubiquitin (polyubiquitin chains) are usually degraded by the 26S proteasome complex. Ubiquitin, a 76 amino acid protein, is conjugated to target proteins through its C-terminal residue (Gly76), which is usually linked to a lysine residue of a target molecule. Substrates can be modified with monoubiquitin or with a polyubiquitin chain that is linked through lysines present in ubiquitin itself. Conjugation involves the sequential actions of three enzymes: a ubiquitin-activating enzyme (E1), a ubiquitin-conjugating enzyme (E2), and a ubiquitin ligase (E3). The E3 is the principal substrate recognition factor (Hershko and Ciechanover, 1998). Although at first suspected to only a small pool of misfolded proteins for degradation by 26S proteasomes, ubiquitin conjugation (ubiquitination) is today recognized as a multifunctional signaling mechanism. Noncanonical functions of ubiquitin are proliferating rapidly and some of the best-characterized are in controlling protein trafficking within the cell (Hicke, 2001).

The similar reactions to the ubiquitin system are utilized in the various kinds of reactions involving the ubiquitin-like proteins (UbLs) that modify substrates for different

purposes than does ubiquitin itself (Hochstrasser, 2000). Such modifications have been discovered in the various ubiquitin-related molecules, such as SUMO-1/Smt3p (Matunis *et al.*, 1996; Johnson *et al.*, 1997; Mahajan *et al.*, 1997), NEDD-8/Rub1p (Osaka *et al.*, 1998; Lammer *et al.*, 1998; Liakopoulos *et al.*, 1998), UCRP (Loeb and Haas, 1992), and Urm1p (Furukawa *et al.*, 2000). Such discoveries suggest that this type of conjugation system serves as a regulatory mechanism in a variety of cellular processes.

Bulk protein degradation in the lytic compartment

The lysosome/vacuole is a single membrane-bound compartment containing various hydrolytic enzymes. The resulting degradation products are reutilized to supply energy and building materials to the cell. All eukaryotic cells contain lysosomes, reflecting the importance of this catabolic organelle. There are several routes to the lysosome for the materials to be degraded in lysosome as follows: Crinophagy is a fusion event between Golgi-derived secretory vesicles with lysosome. Crinophagy is thought to occur for regulation of protein secretion (Lenk *et al.*, 1991). Direct import of cytosolic enzymes to the lysosome has been reported for several specific proteins (Dice, 1990). This process is mediated by recognition of a specific sequence of the target protein by a receptor on the lysosomal membrane and involves the heat-shock protein Hsc73 (Terlecky *et al.*, 1992; Cuervo and Dice, 1996). Microautophagy is defined as the process of incorporation of cytoplasmic components by invagination or engulfment of the lysosomal/vacuolar membrane (Ahlberg and Glaumann, 1985; Mortimore *et al.*, 1988). Macroautophagy (autophagy) is the process by which intracellular membrane structures sequester the cytosol, forming autophagosome, and eventually deliver their contents to lysosomes for degradation.

Macroautophagy (Autophagy)

Autophagy is defined as a process of bulk degradation of cytoplasmic proteins or organelles in the lytic compartment (Schworer *et al.*, 1981; Mortimore *et al.*, 1989; Dunn, 1994). As every eukaryotic cell possesses a lysosome/vacuole system, autophagy seems to be a ubiquitous and basic cellular activity in all eukaryotic cell types. Autophagy has been described mostly in higher eukaryotic cells, such as liver or nerve cells, and differentiating cells or plant cells, by electron microscopy. Segregation of lytic enzymes from the cytosol produces an obvious cell biological problem – how to deliver proteins or organelles destined for degradation into the lumen of this compartment. Autophagy involves the formation of a double-membrane structure, called an autophagosome (Dunn, 1990a), from osmiophilic membranes designated as phagophores (Seglen, 1987; Fengsrud *et al.*, 1995, 2000).

Autophagosome encloses a portion of the cytosol, then fuses with a primary lysosome and matures to become an autolysosome (Dunn, 1990b). The inner membrane structure in the autolysosome is disintegrated, and its contents are digested and recycled to be reused by the cell.

The membrane of the autophagosome could be derived from various sources (Seglen and Bohley, 1992; Mortimore *et al.*, 1996) including the rough endoplasmic reticulum (RER; Dunn, 1990b), a post-Golgi compartment (Yamamoto *et al.*, 1990). The most common interpretation of the available data is that the membrane initially comes from a ribosome-free section of the RER and then assumes the features of the lysosome membrane, losing endoplasmic reticulum (ER) marker proteins as it acquires lysosomal proteins (Dunn, 1990a; Ueno *et al.*, 1991).

Various kinds of investigation on the regulation of autophagy have accumulated information on the individual process of autophagy. The segregation step requires ATP (Plomp *et al.*, 1987) and it is inhibited by incubation at low temperature (Gordon *et al.*, 1987), 3-metyladenine (3MA; Seglen and Gordon, 1982), okadaic acid (phosphatase inhibitor; Holen *et al.*, 1993), and tyrphostins (tyrosine kinase inhibitor; Holen *et al.*, 1993). Blommaart *et al.* reported that 3MA may exert the effect through phosphatidylinositol 3-kinase (PI3-kinase) and other inhibitors of PI3-kinase such as wortmannin and LY294002 also inhibited the autophagy (Blommaart *et al.*, 1997). This suggests that PI3-kinase is involved in the segregation process of autophagy. Through the use of vinblastine, a microtubule depolymerizer, it has long been recognized that microtubules play a role in autophagy (Kovacs *et al.*, 1982). On the contrary, disruption of microtubules by nocodazole treatment retarded the delivery of lysosomal enzymes, but it did not affect the acidification of autophagosome (Aplin *et al.*, 1992). Because the modes of autophagy are so diverse and the physiological role and regulation of autophagy are dependent on the cell type and physiological demands, it is difficult to present a general model for autophagy in higher eukaryotic cells. For this reason, it has been helpful to develop a simple system to elucidate the fundamental machinery of the autophagic process.

Autophagy in yeast

Budding yeast, *Saccharomyces cerevisiae*, is a unicellular eukaryote. A yeast cell has large vacuoles, which is homologous to lysosome in a mammalian cell. The vacuole is an acidic compartment and contains many proteolytic enzymes (Klionsky *et al.*, 1990). It serves as a major storage reserve for basic amino acids, inorganic phosphate and calcium ions (Klionsky *et al*, 1990). The vacuole is the terminal site of most membrane flow within the

cell; it accommodates delivery through numerous pathways and is capable of dynamic membrane rearrangements. Resident hydrolases are delivered to the vacuole from the endosome and Golgi complex as well as from the cytosol. Substrates for degradation arrive from both the cell surface and the cytosol and include entire organelles. When yeast cells were encountered with nutrient starvation, including carbon, nitrogen, phosphorus and sulfur, they respond to their starvation by ceasing growth and entering nonproliferating state as G_1 or G_0 phase of the mitotic cell cycle (Lillie and Pringle, 1980). In the medium containing poor carbon source such as acetate and usually in the absence of nitrogen, cells initiate the meiosis and sporulation (Herskowitz, 1988). The facts that vacuolar proteinase deficient mutants exhibit drastically reduced viability upon nitrogen starvation and that diploids lacking vacuolar proteinases fail to sporulate, indicate the importance of vacuolar proteolysis for the survival and/or differentiation of the organism (Jones, 1984; Kaneko *et al.*, 1982; Teichert *et al.*, 1989; Zubenko and Jones, 1981). In the budding yeast *Saccharomyces cerevisiae*, many of the fundamental processes are analogous to those in higher eukaryotic cells.

Recently, microscopic observation revealed that yeast cells induce autophagy under nutrient starvation. Electron microscopic analyses showed that yeast autophagy occurs in a similar manner to that of mammalian cells (Takeshige *et al.*, 1992; Baba *et al.*, 1994; Baba *et al.*, 1995). So far, yeast autophagy is thought to trace the processes as follows: membrane structure with cup shape appears in cytoplasm under starvation, and then this structure sequesters the cytoplasmic components to become an autophagosome. This autophagosome formation process is accompanied by the assembly of membranous structures (Kirisako *et al.*, 1999). Then the outer membrane of the autophagosome fused with vacuolar membrane and the inner single membrane structure including cytosol is released into the vacuole as autophagic body. Subsequently, the autophagic body and its contents are degraded in a vacuolar-proteinase-dependent manner.

Recent studies revealed that vacuolar protein degradation is also involved in the regulatory mechanisms on catabolite inactivation (Chiang and Schekman, 1991). When glucose-starved cells are cultured in the presence of glucose, the key gluconeogenic enzyme, fructose-1,6-bisphosphatase (FBPase), is selectively targeted from the cytosol to the vacuole for degradation (Chiang and Schekman 1991; Hoffman and Chiang, 1996; Huang and Chiang, 1997). The glucose-induced targeting of FBPase to the vacuole occurs when cells are shifted to glucose from a variety of metabolic conditions such as, acetate, glycerol, galactose and oleate (Chiang *et al.*, 1996). To approach to the targeting mechanism of the FBPase to the vacuole, many *vid* (vacuolar import and degradation deficient) mutants were isolated.

Recently, it was reported that ubiquitination plays important roles in the degradation of FBPase (Shieh *et al.*, 2001).

Methylotrophic yeasts induce peroxisome biogenesis when methanol or oleic acid is the sole carbon source. Excess peroxisomes are specifically degraded if preferred carbon sources such as glucose or ethanol subsequently become available. Analysis of the degradation process by electron microscopy reveals that *Pichia pastoris* utilizes two different mechanisms for pexophagy depending on the specific carbon source (Tuttle and Dunn, 1995). In the presence of ethanol, peroxisomes are degraded by the process of macropexophagy, which is topologically similar to macroautophagy. In contrast, glucose addition triggers a micropexophagic engulfment of peroxisomes directly at the vacuole surface (Tuttle and Dunn, 1995).

These findings suggest that autophagy functions not only for nonselective protein degradation, but also for regulation of metabolic enzyme activity and bulk activity of intracellular organelle under various extracellular environmental changing (Tuttle and Dunn, 1995; Yuan *et al.*, 1997).

Vacuolar protein sorting and autophagy

The biosynthesis of soluble vacuolar glycoproteins in yeast is similar to that of soluble lysosomal glycoproteins in mammalian cells (Kornfeld and Mellman, 1989; Kornfeld, 1992). In both cases newly synthesized precursors enter ER and travel to a late-Golgi compartment. Then the vacuolar proteins are actively sorted away from the compartment. Genetic approaches in yeast have identified more than 40 *VPS* (vacuolar protein sorting) genes required for delivering carboxypeptidase Y (CPY) to the vacuole (Klionsky *et al.*, 1990; Raymond *et al.*, 1992). All the *vps* mutants were classified into six classes from class A to F on the basis of phenotypic criteria, such as vacuolar morphology, vacuolar inheritance to daughter cell, and vacuolar protein localization (Raymond *et al.*, 1992).

The class E *vps* mutants are of special interest as they are characterized by a novel class E compartment. Within the class E compartment, endocytic marker proteins, vacuolar hydrolases and Golgi resident proteins are accumulated (Raymond *et al.*, 1992; Davis *et al.*, 1993; Vida *et al.*, 1993; Piper *et al.*, 1995; Rieder *et al.*, 1996). This suggests that the endocytic protein transport pathway and the Golgi-to-vacuole protein transport converge at this intermediate compartment (Raymond *et al.*, 1992; Piper *et al.*, 1995; Rieder *et al.*, 1996). Functional analyses on the class E *VPS* gene products showed that these proteins are required for outward protein transport from endosome (Piper *et al.*, 1995; Rieder *et al*, 1996; Babst *et al.*, 1997). It was reported that some of *VPS* genes are involved in autophagy. One of the class

E *VPS* genes, *VPS4*, is involved in an autophagic process. Overexpression of a mutant allele ($vps4^{E291K}$) caused dominant effect, namely the overproduced cells induced autophagy constitutively (Shirahama *et al.*, 1997).

Aminopeptidase I transport to the vacuole

The classical model for delivery of hydrolases to the vacuole is via a portion of the secretory pathway. Proteins transit from the endoplasmic reticulum through the Golgi complex, are sorted away from other proteins in the secretory pathway, diverted to the endosome, and then to the vacuole. Analysis of aminopeptidase I (API) and α-mannosidase, which are vacuolar soluble hydrolases, indicate that they are not transported via the secretory pathway (Klionsky *et al.*, 1992; Yoshihisa and Anraku, 1990). It is constitutively synthesized as an inactive precursor form (proAPI) in the cytosol. It is targeted to the vacuole and then processed by vacuolar proteinase at its N-terminal region to become mature (mAPI; Segui-Real *et al.*, 1995).

After synthesis, proAPI rapidly oligomerizes in the cytosol into a dodecamer (Kim *et al.*, 1997), then the complex (Cvt complex) was surrounded by autophagosome-like double membrane structure and the outer membrane fuses with vacuolar membrane to release the inner membrane structure including the Cvt complex into the vacuole (Scott *et al.*, 1997; Baba *et al.*, 1997). A density gradient centrifugation analysis showed that proAPI transits to and enters the vacuole as a dodecamer (Kim *et al.*, 1997). The fact that dodecameric proAPI is approximately 732kDa in mass argues against translocation through a proteinaceous channel. API uses an alternate targeting mechanism, the Cvt pathway.

A genetic screen was used to identify factors involving the Cvt pathway. Wild-type cells accumulate primarily mature API because the protein is stable in the vacuole, in agreement with its role as a resident hydrolase. The basis of the mutant screen was the detection of accumulated precursor API (Harding *et al.*, 1996). The *cvt* mutants include mutations in genes for processing enzymes such as proteinase B, as well as certain *VPS* genes. Proteinase B is required in the vacuole for processing proAPI to the mature form. Most of the *cvt* mutants, however, do not affect transit through the secretory pathway.

Genetic analysis of autophagy in yeast

Autophagosomes, which are generated in the cytoplasm by starvation, fuses with the vacuole releasing the inner vesicle to become single-membrane autophagic bodies. Autophagic bodies are degraded in a proteinase B-dependent manner. In the presence of

phenylmethylsulfoyl fluoride (PMSF), which inhibits proteinase B, starved cells accumulate autophagic bodies in vacuoles. This accumulation of autophagic bodies can be easily monitored under the light microscope. Taking advantage of the morphological criteria, 14 mutants defective in autophagy (*apg*) were isolated in *S. cerevisiae* (Tsukada and Ohsumi, 1993). Recently, *APG17* was obtained by two-hybrid screening (Kamada *et al.*, 2000). These mutants could not accumulate autophagic bodies in starvation medium containing PMSF. They also showed reduced viability under starvation, and homozygous diploid of *apg* mutants were defective in sporulation (Tsukada and Ohsumi, 1993). These suggest that autophagic degradation of cytosolic components is indispensable for cells to keep their viability under starvation and to supply sufficient materials for sporulation. Extensive electron microscopic analyses revealed that *apg* mutants accumulated no autophagosome in their cytosol under starvation conditions, suggesting that *APG* genes are involved in the autophagosome formation or earlier steps of autophagy, rather than in autophagosome fusion to the vacuole.

The other genetic approach to identify autophagy mutants based on the decrease of specific enzymes following starvation. Fatty acid synthase was used as a marker for this purpose (Thumm *et al.*, 1994). This cytosolic enzyme is effectively degraded in the vacuole in a Pep4p-dependent manner. Mutants were identified that accumulated fatty acid synthase under starvation conditions. A second screen was based on the inability to accumulate autophagic bodies. Through this approach, three *aut* mutants (autophagocytosis) were obtained (Thumm *et al.*, 1994). By expanding the procedure, additional *aut* mutants were isolated (Harding *et al.*, 1996).

Complementation studies reveal that the *apg* mutants overlap with the two sets of mutants, the *aut* and *cvt* mutants. All *apg* mutants except *apg17* are shown to be defective in the Cvt pathway, indicating that autophagy and the targeting of API to the vacuole share common molecular mechanisms. Macroautophagy is a vesicle-mediated process that could accommodate import of the proAPI oligomer. In addition, macroautophagy machinery is essential for the selective delivery of excess peroxisomes to the vacuole by the related pexophagy pathway (for review see Kim and Klionsky, 2000).

Characterization of APG *genes*

Recent characterization of the Apg proteins has identified two ubiquitin-like systems utilizing approximately half of the Apg proteins. Apg12p, a ubiquitin-like protein, is covalently attached to Apg5p to form an Apg12p-Apg5p conjugate controlled by the serial action of Apg7p and Apg10p (Mizushima *et al.*, 1998). Apg7p, a member of the E1-like activating enzymes, forms a thioester linkage with Apg12p (Tanida *et al.*, 1999; Kim *et al.*,

1999; Yuan *et al.*, 1999). Apg12p subsequently forms a thioester intermediate with Apg10p, an E2 conjugating enzyme (Shintani *et al.*, 1999). Apg12p is then linked to Lys149 of Apg5p through an isopeptide bond with the C-terminal glycine. Apg16p then interacts through its C-terminal coiled-coil region to form homo-oligomers following the direct interaction with the Apg12p-Apg5p conjugate (Mizushima *et al.*, 1999). In mammalian cells, a homologue of the Apg12p-Apg5p conjugate transiently associates with the membranes of precursor autophagosomes (Mizushima *et al.*, 2001).

Aut7p/Apg8p, a second ubiquitin-like protein involved in autophagy, is conjugated to phosphatidylethanolamine (Aut7p-PE) by the serial action of three Apg proteins, Aut2p/Apg4p, Apg7p and Aut1p/Apg3p (Kirisako *et al.*, 2000; Ichimura *et al.*, 2000). The C-terminal Arg117 of Aut7p is removed through the action of Aut2p, a cysteine protease (Kirisako *et al.*, 2000), to expose Gly116. Following activation by Apg7p (E1), the processed Aut7p is transferred to Aut1p (E2). Aut7p is then covalently linked to phosphatidylethanolamine. Aut2p further cleaves Aut7p-PE, releasing Aut7p, an essential step in the normal progression of autophagy (Kirisako *et al.*, 2000). Aut7p is the first protein to localize to autophagosomes and intermediate structures (Kirisako *et al.*, 1999; Huang *et al.*, 2000); this characteristic of Aut7p allows us to use Aut7p to monitor autophagosome formation. LC3, the mammalian homologue of Aut7p, is also localized on the membranes of autophagosomal and precursor membranes (Kabeya *et al.*, 2000; Mizushima *et al.*, 2001).

Additional Apg proteins, not known to participate in ubiquitin-like systems, are also required for autophagy. Vps30p/Apg6p, in addition to a role in autophagy, functions in vacuolar protein sorting (Kametaka *et al.*, 1998). Vps30p forms a specific PI3-kinase complex required for autophagy, consisting of Vps30p, Apg14p, Vps34p and Vps15p. This data suggests that the dynamic membrane events mediated by the PI3-kinase complex are necessary for autophagy (Kihara *et al.*, 2001a). A class of PI3-kinase and beclin, a human homologue of Vps30p, are also essential for autophagy in human cells (Liang *et al.*, 1999; Petiot *et al.*, 2000). Beclin physically interacts with the PI3-kinase complex on the *trans*-Golgi network (Kihara *et al.*, 2001b).

Tor-kinase negatively regulates the induction of autophagy; this kinase activity is inhibited by rapamycin (Noda and Ohsumi, 1998). As the inactivation of Tor activity induces autophagy, treatment with rapamycin mimics the starvation response. The inactivation of Tor activity causes a rapid dephospholylation of Apg13p (Kamada *et al.*, 2000; Abeliovich *et al.*, 2000). Apg13p and Apg17p associate with Apg1p protein kinase to form the Apg1p protein kinase complex (Kamada *et al.*, 2000), an essential component of autophagy. Binding of

dephosphorylated Apg13p to this complex enhances the kinase activity of Apg1p (Kamada *et al.*, 2000).

The aim of this study

The characteristics of each Apg protein are gradually being uncovered; their functional interrelationship, however, is poorly understood (Figure 1). This is due to a lack of markers allowing the identification of intermediate steps occurring before or during autophagosome formation. To obtain further insights into the functional relationship between the Apg proteins, I observed the behavior of Apg proteins fused to fluorescent proteins utilizing a sensitive imaging system. I examined the dynamics of the Apg proteins involved in the two ubiquitin-like systems, Apg5p and Aut7p. Based on their modification and localization in *apg* mutants, I have defined a pre-autophagosomal structure containing Apg1p, Apg2p, Apg5p, Aut7p and Apg16p. This structure, involved in the production of autophagosomes, provides a clue for investigating the steps of autophagosome formation.

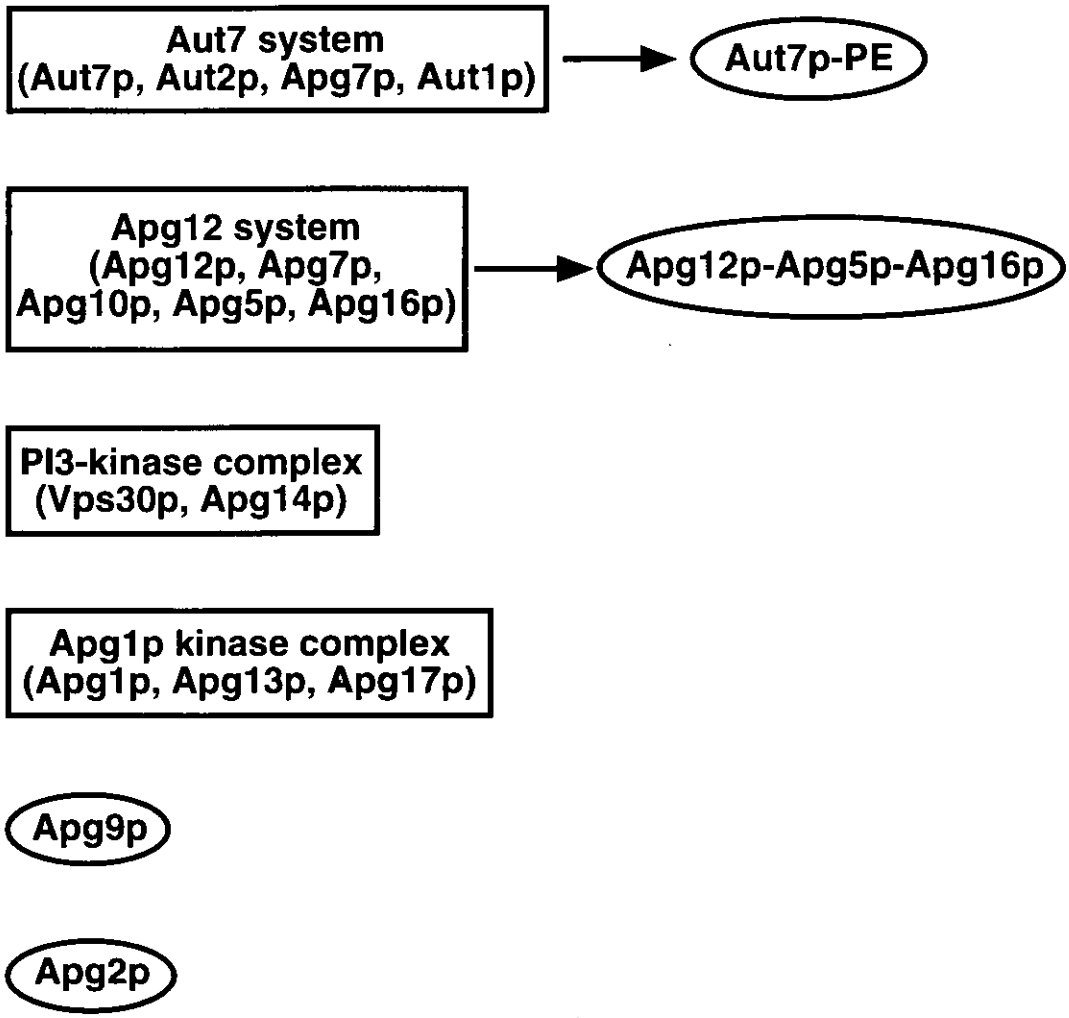

Figure 1. Complexes and reactions described in Apg proteins. Every Apg protein is involved in autophagosome formation but a comprehensive understanding of the overall network is missing. See the text for details.

Materials and methods

Yeast Strains and Media

Yeast strains used in this study are listed in Table I. I used standard methods for yeast manipulation (Kaiser *et al.*, 1994). Cells were grown in either YEPD (1% yeast extract, 2% peptone and 2% glucose) or SD + CA medium (0.17% yeast nitrogen base w/o amino acid and ammonium sulfate, 0.5% ammonium sulfate, 0.5% casamino acid and 2% glucose) supplemented with 0.002% adenine sulfate, 0.002% tryptophan and 0.002% uracil if necessary. Autophagy was induced in growth media containing either 0.5 or 1 μg/ml rapamycin (Sigma). To induce nitrogen starvation, the cells were incubated in SD (-N) medium (0.17% yeast nitrogen base w/o amino acid and ammonium sulfate, and 2% glucose). Yeast extract, yeast nitrogen base w/o amino acid and ammonium sulfate and casamino acid were obtained from Difco. Peptone, glucose, ammonium sulfate, adenine sulfate, tryptophan and uracil were purchased from Wako pure chemical industries, Ltd.

Plasmids

In this study, centromeric plasmids were used to produce physiological levels of expression. The pRS316 GFP-AUT7 plasmid was created by substituting the 3 X hemagglutinin (HA) sequence immediately after the start codon of the *AUT7* open reading frame (ORF) in pTK108 (Kirisako *et al.*, 1999) with a modified GFP sequence (S65T), following digestion by *BamHI*. The pRS316 GFP-AUT7FG plasmid was created by substituting the 3 X myc sequence immediately after the start codon of the pRS316 AUT7FG (Kirisako *et al.*, 2000). The pRS314 ECFP-AUT7 plasmid was created by cloning an enhanced CFP (ECFP) fragment, amplified from pECFP (Clontech), into pRS316 GFP-AUT7 digested with *BamHI*. From the resulting pRS316 ECFP-AUT7, I subcloned an excised *SacI-XhoI* fragment into pRS314. The pRS314 APG5-GFP and the pRS416 APG9-GFP plasmids were the generous gifts of Dr. D. J. Klionsky (University of Michigan). Site-directed mutagenesis using QuikChange™ (Stratagene) was utilized to insert a *BamHI* site into pYAPG507, immediately before the stop codon of the *APG5* ORF (Kametaka *et al.*, 1998) to create the pRS316 APG5-EYFP plasmid. An enhanced YFP (EYFP) fragment was amplified from pEYFP (Clontech), digested with *BamHI*, and cloned into the *BamHI* site of pYAPG507.

The pRS316 YFP-APG1 plasmid was created by inserting the *BamHI* cassette of EYFP immediately after the start codon of the *APG1* ORF. Site-directed mutagenesis then

inserted a *BglII* site using QuikChange™. The pRS316 GFP-APG1^{ts} plasmid was created by inserting the *BamHI* cassette of S65T immediately after the start codon of the *APG1*^{ts} ORF. Site-directed mutagenesis then inserted a *BglII* site using QuikChange™. The pRS314 APG16-YFP plasmid was created by inserting the *NotI* cassette of EYFP immediately before the stop codon of the *APG16* ORF (Mizushima *et al.*, 1999).

Generation of the* apg1^{ts} *allele

APG1 was mutagenized by previously described PCR procedures (Cadwell and Joyce, 1995). The mutagenized gene was co-transformed into YYK190 cells with a gapped pRS316 plasmid, containing portions homologous to both ends of the PCR product. Two hundred four transformants were picked and patched onto YEPD plates, which were then incubated overnight at temperatures of 30°C and 37°C. Cells were then subjected to treatment with 0.4 μg/ml rapamycin at each temperature. I examined the generation of autophagic bodies under a phase-contrast microscope. Plasmids recovered from the 22 candidates that passed the initial screening were used to re-transform YYK190 cells to confirm the temperature-sensitive phenotype.

Eight strains that passed the initial screening were subjected to an ALP assay to quantify autophagic activity. YYK126 cells were transformed with each candidate plasmid. Cells were cultured in YEPD medium at 23°C; ALP activities were measured after a 6 h nitrogen starvation at 23°C or 37°C. Five strains were finally confirmed as temperature sensitive mutants. Two of the five strains exhibiting clear temperature sensitivity were used for further analysis. The plasmids recovered from these two strains possessed identical sequences. This allele was used as *apg1*^{ts}. The temperature sensitivity resulted from the following amino acid substitutions: L88H, F112L and S158P.

Generation of a strain expressing API-GFP

I constructed a strain expressing API-GFP with a PCR-based gene modification method (Longtine *et al.*, 1998), which inserts the S65T sequence directly to the target gene. A sequence of GFP-kanMX6, containing sequences homologous to 3' end of API gene, was amplified from the pFA6a-GFP(S65T)-kanMX6 plasmid (Longtine *et al.*, 1998), transformed to SEY6210 cells and plated onto YEPD plates. The plates were incubated overnight at 30°C, and then replicated onto YEPD plates containing 400 μg/ml G418 (Gibco). Colonies were picked and grown in YEPD medium and the integration was checked by PCR analysis. Cells

expressing API-GFP were subjected to immunoblot analysis and fluorescence microscopy as described above.

Immunoblot Analysis

To detect either the GFP-Aut7p or Apg12p-Apg5pGFP conjugate, lysates were prepared from cells grown in SD + CA medium to a density of approximately OD_{600} =1 by NaOH/2-mercaptoethanol extraction with a slight modification (Horvath and Reizman, 1994). Briefly, anti-Aut7p antiserum (Kirisako *et al.*, 2000) and anti-Apg12 antiserum (Ishihara, unpublished result), respectively, were used as the primary antibodies. To detect Apg1p, API and free GFP, I utilized anti-Apg1p antiserum (Matsuura *et al.*, 1997), anti-aminopeptidase I antiserum (gift from Dr. D. J. Klionsky) and anti-GFP antiserum (gift from Dr. Abe) as the primary antibodies, respectively. Aut7p-PE was detected following SDS-PAGE in the presence of 6 M urea, as described (Kirisako *et al.*, 2000). I collected cells that had been either grown in YEPD medium to a density of approximately OD_{600} =1 or then starved in SD (-N) medium. Harvested cells were then washed with distilled water and disrupted with glass beads (Sigma) for 5 min in a buffer containing 50 mM Tris-HCl (pH 7.5), 150 mM NaCl, 5 mM EDTA, 5 mM EGTA, 1 mM PMSF (Sigma) and a protease inhibitor cocktail (Complete; Roche) at 4 °C. Cell lysates were boiled in SDS sample buffer for 5 min. Equal protein amounts (20 μg protein) were subjected to electrophoresis, transferred to PVDF membrane (Millipore) and detected with a combination of anti-Aut7p antibody and peroxidase-conjugated goat anti-rabbit IgG antibody (Jackson Immunoresearch Laboratories, Inc.) by ECL system (Amersham Pharmacia Biotech). Protein concentration was measured using a BCA reagent kit (Pierce) with BSA as a standard.

Fluorescence Microscopy

Recently, several reports addressed the localization of GFP-tagged Apg proteins. However, those images were obtained by overexpressing the fusion proteins. As overexpression of GFP-tagged proteins often disturbs the inherent localization of the proteins, centromeric expression levels are desirable. Recent advance in fluorescence microscopy and improvement of imaging detectors provide a new tool to detect weaker fluorescent signals. Therefore, I introduced a DeltaVision microscope system (Applied Precision) equipped with a sensitive CCD camera and electronic shutters that prevent living cells from photodamages. Culture temperatures were controlled with a ΔTC3 culture dish system (Bioptechs) during time-lapsed video microscopy. FM4-64 (Molecular Probes) was used to identify the vacuolar

membrane under a fluorescence microscope. The stock solution of FM4-64 was prepared at a concentration of 1 mg/ml in dimethylsulfoxide (DMSO). Growing cells were incubated with 1 μg/ml FM4-64 for 15 min and then chased 30 min at 30°C. The labeled cells were visualized by fluorescence microscopy using a Texas Red filter. To observe GFP-tagged proteins under a fluorescence microscope, I employed a FITC filter. A dual band filter set for CFP and YFP (86002; Chroma Technology Corp.), was used to detect the localization of CFP- and YFP-tagged proteins.

Immunofluorescence microscopy was performed as described previously (Nishikawa *et al.*, 1994). Cells harboring the APG9-GFP plasmids were grown in SD + CA medium to a density of approximately OD_{600} = 1.5. Cultures were then treated with 0.5 μg/ml rapamycin for 2 h and subsequently fixed in 5% formaldehyde. Cells were then converted into spheroplasts and permeabilized with PBS containing 0.5% Triton-X100 for 10 min at room temperature. Next, the cells were dropped onto multiwell slide glasses (Cel-line Associates), pre-coated with polylysine (Sigma). Affinity-purified anti-Aut7p antibody was used as the primary antibody, followed by incubation with the Cy™5-conjugated secondary antibody (Amersham). For double labeling with GFP-tagged proteins, I used Cy5, a fluorescent dye (Ex: 649 nm and Em: 670 nm), to minimize the bleeding of the fluorescence into the GFP channel (Ex: 489 nm and Em: 511 nm). GFP and Cy5 were visualized with the FITC and the Cy5 filter sets, respectively.

Electron Microscopy

Cells were grown in SD + CA medium to a density of approximately OD_{600} = 1.5. Cultures were then treated with 0.2 μg/ml rapamycin for 6 h and subsequently harvested, sandwiched between two aluminum disks (LZ02136VN, BAL-TEC, Principality of Liechtenstein), and quickly frozen by a high-pressure freezing machine (HPM010S, BAL-TEC). The cells were kept in acetone below –80 °C for 3 days and then gradually warmed to 4 °C. The cells were placed in propylene oxide and then embedded in LR White resin (London Resin Company Ltd.). The resin was polymerized with TUV-100 (Dohan EM) at 4 °C. Thin sections were cut with a diamond knife (Diatome) in a Ultracut T (Leica) and collected onto formvar coated nickel grids (Thinbar). The glids were incubated with monoclonal anti-HA ascites (16B12, BAbCO) and/or affinity purified Apg2p (Shintani *et al.*, 2001) and labeled with 5 or 10 nm-gold conjugated goat anti-mouse and/or anti-rabbit IgG (BB International, UK). The grids were then stained with 3% uranyl acetate for 10 min and

with lead citrate for 20 sec, and examined under a JEOL 1200EX electron microscope at an acceleration voltage of 80 kV.

Alkaline phosphatase (ALP) assay

Autophagic activities were estimated by measuring alkaline phosphatase activity in cells expressing a cytosolic proform of the phosphatase (Pho8Δ60p; Noda *et al.*, 1995). α-naphtyl phosphate (Sigma) was used as a substrate. Pho8Δ60p is transported to the vacuole via autophagy and processed in the vacuolar lumen to become active.

Results

GFP-Aut7p labels autophagosomes and autophagic bodies

Electron microscopic analysis has shown that Aut7p is localized on autophagosomes and autophagic bodies (Kirisako *et al.*, 1999). First, I checked whether N-terminally GFP-tagged Aut7p is capable of labeling these structures. GFP fusions were expressed from centromeric plasmids under the control of authentic promoters. In Δ*aut7* cells expressing physiological levels of a GFP-Aut7p fusion protein (Figure 2A), GFP-Aut7p complemented the defect of autophagy (Figure 2B-D).

Next, I examined accumulation of autophagosomes using the Δ*ypt7* mutant (Kirisako *et al.*, 1999). In my experiments, I induced autophagy by rapamycin, since it mimics the starvation response even in a rich medium (Noda and Ohsumi, 1998). During vegetative growth, mostly one punctate structure per cell was observed in the Δ*ypt7* cells expressing GFP-Aut7p (Figure 3A). As expected, many dots appeared in every cell after rapamycin treatment (Figure 3B), indicating these dots were autophagosomes. Here, autophagosomes were visualized under a fluorescence microscope in living cells. Autophagosomes fuse with the vacuole and enter the vacuolar lumen to become autophagic bodies. The proteinase A deficient mutant (Δ*pep4*) fails to degrade autophagic bodies. Hence, the mutant accumulates autophagic bodies in the vacuole during autophagy. In Δ*pep4* cells, autophagic bodies were stained with GFP-Aut7p (Figure 3C). GFP-Aut7p labels the known autophagic organelles, i. e. autophagosomes and autophagic bodies.

Next I examined distribution of GFP-Aut7p in Δ*aut7* cells under growing and starving conditions. GFP-Aut7p was detected in the form of a punctate structure close to the vacuole during vegetative growth, (Figure 3D-G). After rapamycin treatment, the punctate structure became brighter (arrow in Figure 3H). Within 1 h after incubation with rapamycin, dots with less intensity appeared in the cytosol in addition to the punctate structure (arrowheads in Figure 3H). It is likely that these dots represent autophagosomes. At 5 h after the treatment, the vacuole was filled with green fluorescence (Figure 3I) and the punctate structure was still observable close to the vacuole (arrow in Figure 3I). The GFP portion transported to the vacuole was relatively stable. In *apg* mutants, the vacuolar lumen was not stained with GFP after the treatment with rapamycin (see Figure 11B, 4 min), indicating that Aut7p was routed into the vacuoles via autophagy. Here, I provide a visual demonstration that the contents of autophagic bodies diffused throughout the vacuole as a consequence of the disintegration of membranes of autophagic bodies. Taken together, GFP-Aut7p labels the following structures:

autophagic bodies (Figure 3C), autophagosomes (Figure 3C and arrowheads in 3H), and a functionally unknown punctate structure close to the vacuole (arrows in Figure 3G-I).

Several Apg proteins are converged to the punctate structure

Apg proteins are involved in several essential reactions in autophagy, such as ubiquitin-like systems or phosphorylation reactions. The interrelation between these reactions in autophagosome formation, however, remains unknown. It is critical to know the intracellular localization. Several Apg proteins, e. g. Apg5p (George *et al.*, 2000), Aut7p/Apg8p (Kim *et al.*, 2001) and Apg9p (Noda *et al.*, 2000), are localized to perivacuolar punctate structures. To analyze the localization of Apg proteins to these punctate structures, I visualized GFP-fused Apg proteins using a sensitive microscope system. GFP fusions were expressed from centromeric plasmids under the control of natural promoters. Apg5p-GFP retained the ability to conjugate with Apg12p (Figure 4A); when introduced into deficient cells, Apg5p-GFP restored proper autophagic function (Figure 4B and C). The additional chimeric proteins used in this study were also functional in autophagic process (data not shown).

I fused cyan fluorescent protein (CFP) and yellow fluorescent protein (YFP) to several different Apg proteins and examined their colocalization. Fluorescent Aut7p served as a marker of the punctate structures. Apg1p, Apg5p and Apg16p colocalized with Aut7p on a single punctate structure located close to the vacuole (Figure 5). After the addition of rapamycin, CFP-Aut7p was delivered to vacuoles in a time-dependent manner (Figure 5A, D and G). YFP-Apg1p was delivered to vacuoles after the lengthy treatment with rapamycin (data not shown), whereas Apg5p-YFP and Apg16p-YFP were never transported to the vacuoles (Figure 5B and H). Apg2p colocalizes with Aut7p on a perivacuolar punctate structure but does not stain autophagosomes (Shintani *et al.*, 2001). Consequently, the punctate structure is shown to contain Apg1p, Apg2p, Apg5p, Aut7p and Apg16p. As Apg13p and Apg17p interact physically with Apg1p (Kamada *et al.*, 2000), it is probable that these molecules also reside on the punctate structure.

Apg9p is a putative membrane protein and is not cofractionated with typical endomembrane marker proteins, autophagosomes or Cvt vesicles (Noda *et al.*, 2000). Apg9p-GFP exhibited an uneven, cytosolic distribution in addition to its localization on several punctate structures (Noda *et al.*, 2000; Figure 6A and B). This pattern was not altered in other *apg* mutants (Figure 6C and D; data not shown). To examine whether this protein is utilized as a punctate structure marker, I compared the localization of Apg9p-GFP and Aut7p by immunofluorescence microscopy. The punctate structures labeled with Aut7p seldom

colocalized with those labeled by Apg9p-GFP (Figure 6E-L), although the two structures were occasionally in close proximity (arrows in Figure 6K). This pattern of Apg9p indicates that it is not a suitable marker for the punctate structure.

Next, I examined the localization of Apg5p-YFP and CFP-Aut7p in Δ*ypt7* cells. Following rapamycin treatment of these cells, autophagosomes labeled with CFP-Aut7p appeared as dim dots in the cytosol (Figure 7A), whereas Apg5p-YFP was detected as a punctate pattern (arrow in Figure 7B). Every punctate structure labeled with Apg5p-YFP was associated with CFP-Aut7p (arrow in Figure 7C). CFP-Aut7p staining of the structure was of a greater intensity than the other CFP-Aut7p dots (arrow in Figure 7A). These observations suggest that this punctate structure containing several colocalized Apg proteins is not an autophagosome. Apg2p shows a similar pattern to Apg5p (Shintani *et al.*, 2001), indicating that Apg2p and Apg5p are useful for the markers of the punctate structure.

To investigate the involvement of the endocytic pathway in punctate structure formation, I examined the class E compartment, an exaggerated prevacuolar compartment in class E vacuolar protein sorting (*vps*) mutants (Raymond *et al.*, 1992). The class E compartment is labeled with FM4-64, a lipophilic stylyl dye, as an intensely stained membrane-enclosed structure (Vida and Emr, 1995) and morphologically similar to the punctate structure labeled with Aut7p. I observed the localization of GFP-Aut7p in one of the class E *vps* mutants, Δ*vps4* (Raymond *et al.*, 1992). The GFP-Aut7p punctate structure did not colocalize with the class E compartment in this mutant (Figure 8). These data suggest that the punctate structure is not organized through the endocytic pathway. Therefore, this punctate structure is a novel structure localized proximal to the vacuole.

Analysis of apg1^{ts} *mutant provides evidence that the punctate structure is involved in autophagosome formation*

I have found a novel punctate structure in which several Apg proteins are concentrated. Therefore, I surveyed whether each *APG* gene is required for the organization of the punctate structure. I noticed that the structure was detected normally in the Δ*apg1* cell (Figure 9). This result suggests that the *APG1* gene is involved not in the organization of the punctate structure but in autophagosome formation. To examine if the punctate structure is physiologically functional, I generated an *apg1*^{ts} allele by polymerase chain reaction (PCR) mutagenesis. Autophagic activities were measured by monitoring the alkaline phosphatase (ALP) activity in cells expressing a cytosolic proform of the ALP (Pho8Δ60p), which is transported to the vacuoles by autophagy and becomes mature (Noda *et al.*, 1995). I estimated

the temperature sensitivity of this allele from the maturation of API (Figure 10A) and the ALP assay (Figure 10B) using Δ*apg1* cells carrying the apg1^{ts} plasmid (*apg1*^{ts} cells). At 23°C, the *apg1*^{ts} cells contained normal levels of mature API (Figure 10A) and possessed significant autophagic activity (Figure 10B). At 37°C, however, both the maturation of API and autophagic activity were completely blocked (Figure 10A and B). Autophagy in the *apg1*^{ts} cells at 30°C was occurred at the same levels as at 23°C. The activity of ALP increased linearly with time for 6 h following incubation in a nitrogen free medium at 23°C (Figure 10C). Upon transferring the cells to 37°C, autophagy was blocked (Figure 10C). When the cells were transferred from 37°C to 23°C, the autophagic activity was recovered without a lag period (Figure 10C). Apg1^{ts}p was detectable by immunoblot even after an overnight incubation at 37°C (Figure 10A), demonstrating that *apg1*^{ts} is a reversible temperature sensitive allele defective in autophagy. Conformational change of Apg1^{ts}p might be crucial for the temperature sensitivity.

Upon temperature shift from 37°C to 30°C, I followed the dynamics of GFP-Aut7p in *apg1*^{ts} cells. At 30°C, GFP-Aut7p was visualized in the punctate structure and the vacuole after rapamycin treatment, as seen in wild-type cells (Figure 11A). At 37°C, the staining intensity of the punctate structure increased accompanied by a lack of vacuolar staining after rapamycin treatment (Figure 11B, 4 min). Next, I examined the progression of GFP-Aut7p staining following temperature decrease in real-time using time-lapse microscopy. Within 10 minutes, several dots labeled with GFP-Aut7p separated from the punctate structure (Figure 11B). In 30 minutes of incubation at 30°C, fluorescence intensity of vacuoles became brighter as these dots disappeared, suggesting they are autophagosomes. Therefore, I concluded that the punctate structure actually participates in the formation of autophagosomes.

I next treated the *apg1*^{ts} cells with 10 μg/ml cycloheximide for 20 min, following a 4 h incubation at 37°C in the presence of rapamycin. Upon temperature decrease, similar dots appeared, leading to fluorescent staining of the vacuole (data not shown). This experiment demonstrates that the emergence of autophagosomes from the punctate structure depends on the activity of Apg1p; *de novo* protein synthesis, however, is not necessary. As Apg1p or Apg1^{ts}p is localized to the punctate structure (Figure 5D-F and data not shown), the Apg1p protein kinase complex functions in autophagosome formation at a later step than the organization of the structure. I therefore designated this punctate structure as the "pre-autophagosomal structure".

Ultrastructure of the pre-autophagosomal structure

To characterize the ultrastructure of the pre-autophagosomal structure, immunoelectron microscopy was performed. Aut7p is localized on autophagosomes, autophagic bodies (Kirisako *et al.*, 1999) and the pre-autophagosomal structure (Figure 5A, D and G). To detect autophagosomes, Aut7p was used as a marker. Δ*aut7* cells expressing N-terminally 3 X HA-tagged Aut7p were treated with rapamycin for 6 h. Aut7p was detected with the anti-HA antibody. As previously described, Aut7p localized in the lumen of autophagosomes (Figure 12A), both sides of circular isolation membranes under course of autophagosome formation (Figure 12B) and a small electron-dense area close to the vacuole (Figure 12C). Next, to label the pre-autophagosomal structure specifically, Apg2p was stained with an affinity-purified anti-Apg2 antibody (Shintani *et al.*, 2001). Similar to Aut7p, Apg2p localized to an electron dense region proximal to the vacuole (Figure 12D). However, the signals of Apg2p were never detected in autophagosomes (data not shown) or the circular isolation membrane of autophagosome (arrowheads in Figure 12E and F). This result is supported by the observation under a fluorescence microscope that Apg2p does not localize on autophagosomes (Shintani *et al.*, 2001). Instead, gold particles were localized outside of such a membrane (Figure 12E) or on a structure next to one edge of the circular isolation membrane (Figure 12F). To confirm the pre-autophagosomal structure, Aut7p and Apg2p were simultaneously labeled with different sizes of gold particles. In accordance with the above observations, Aut7p and Apg2p were concentrated to an electron-dense region close to the vacuole (Figure 13A). A previous study showed that Aut7p first localizes on the circular isolation membrane of autophagosome but transferred to the autophagosomal lumen as autophagosome matures (Kirisako *et al.*, 1999). During the process of autophagosome formation, Aut7p and Apg2p showed discrete microlocalizations: Aut7p was localized on the circular isolation membrane (arrowheads in Figure 13B) or the lumen of autophagosome (arrowheads in Figure 13C and D) whereas Apg2p was concentrated to an open area of isolation membranes (arrows in Figure 13B and C) and appeared to localize on membrane-like structures (arrows in Figure 13C). These results suggest that the pre-autophagosomal structure is localized close to the isolation membrane of autophagosome and specifically labeled with Apg2p. I showed that the pre-autophagosomal structure is localized next to the isolation membrane during autophagosome formation, further investigation of the pre-autophagosomal structure is possible by conventional electron microscopy.

APG *genes required for the organization of the pre-autophagosomal structure*

I have identified the pre-autophagosomal structure in which several Apg proteins are concentrated and demonstrated that it plays a crucial role for autophagosome formation. I examined the organization within this structure by studying the localization of Apg5p-GFP and GFP-Aut7p in *apg* mutants (Figure 9; summarized in Table II). I also assessed the quantities of phosphatidylethanolamine-conjugated Aut7p (Aut7p-PE; Kirisako *et al.*, 2000; Ichimura *et al.*, 2000) in each *apg* mutant by SDS-PAGE in the presence of 6 M urea (Figure 14). Based upon these observations, I grouped the *apg* mutants into three categories. These classes corresponded well to defined functional units, including the Apg1p protein kinase complex, the two ubiquitin-like systems and the PI3-kinase complex necessary for autophagy. This classification provides several new insights into the interaction between these classes, detailed in the following sections.

Class A apg *mutants are not involved in the organization of the pre-autophagosomal structure*

The class A mutants possess both Apg5p-GFP and GFP-Aut7p localized to the pre-autophagosomal structure as in wild-type cells (Table II). The class A genes consist of *APG1*, *APG2*, *APG13* and *APG17*. Apg13p and Apg17p are regulatory factors of the Apg1p protein kinase. As the class A mutants demonstrate normal punctate structures, the Apg1p protein kinase complex is unlikely to be involved in the formation of the structure. The class A mutants all possessed normal levels of Aut7p-PE (Figure 14).

Class B apg *mutants have a defect in the localization of Aut7p on the pre-autophagosomal structure*

In class B mutants, Δ*aut1*, Δ*aut2*, Δ*apg5*, Δ*apg7*, Δ*apg10* and Δ*apg12*, Apg5p-GFP was detected on the pre-autophagosomal structure; GFP-Aut7p was not. Interestingly, these are the genes involved in the two ubiquitin-like conjugation systems: the Aut7 system (Δ*aut2*, Δ*apg7* and Δ*aut1*) and the Apg12p-Apg5p conjugation system (Δ*apg12*, Δ*apg7*, Δ*apg10* and Δ*apg5*). In Δ*apg1*Δ*apg7* double mutant, GFP-Aut7p did not localize to the pre-autophagosomal structure (Table II). This result demonstrates that *APG7* (class B) is epistatic to *APG1* (class A) for the localization of Aut7p, suggesting that the class B *APG* genes govern the localization of Aut7p to the pre-autophagosomal structure prior to class A genes function. As previously reported, mutants of the Aut7 system lacked detectable Aut7p-PE (Figure 14; Ichimura *et al.*, 2000). These studies demonstrated that the localization of GFP-

Aut7p to the pre-autophagosomal structure is tightly coupled to the Aut7p lipidation. The association of Aut7p with the pre-autophagosomal structure occurs with the PE-conjugated form. In *Δaut1* or *Δaut2* mutant, the Apg12p-Apg5p conjugate is formed normally (Mizushima *et al.*, 1998); Apg5p-GFP was localized on the pre-autophagosomal structure, as seen in wild-type cells (Table II). Therefore, the lipidation of Aut7p is essential for the localization of Aut7p but not required for localization of (Apg12p-)Apg5p to the pre-autophagosomal structure.

Interestingly, Apg5p-GFP was detected on the pre-autophagosomal structure in mutants of the Apg12 system (*Δapg12* and *Δapg10*; Table II), suggesting the conjugation of Apg12p is not necessary for Apg5p localization. On the other hand, in Apg12 system mutants (*Δapg12*, *Δapg10* and *Δapg5*), I could not detect GFP-Aut7p on the pre-autophagosomal structure (Table II). In addition, these mutants demonstrated severely reduced levels of Aut7p-PE (Figure 14). A defect in the membrane association of Aut7p in Apg12p conjugation mutants (Kim *et al.*, 2001) may be explained by decreases in the total level of Aut7p-PE in the absence of the conjugate.

To examine the effects of the disruption of the Apg12p-Apg5p conjugate on Aut7p localization, I estimated the levels of Aut7p-PE in *Δaut2* cells expressing the carboxy-terminal processed form of Aut7p (Aut7FGp; Ichimura *et al.*, 2000; Kirisako *et al.*, 2000). Aut2p/Apg4p, a cysteine protease, is essential for Aut7p processing and Aut7p-PE deconjugation. Aut7p-PE accumulates in *Δaut2* cells expressing Aut7FGp because the inability of these cells to deconjugate Aut7p-PE (Kirisako *et al.*, 2000). The levels of Aut7p-PE in *Δaut2Δapg10* and *Δaut2Δapg12* cells were reduced from the levels in *Δaut2* cells, but Aut7p-PE was actually generated in *Δaut2Δapg10* and *Δaut2Δapg12* cells (Figure 15). This result indicates the Apg12p-Apg5p conjugate is not essential for Aut7p-PE formation. I then constructed a GFP-AUT7FG plasmid, which I expressed in *Δaut2Δapg10* and *Δaut2Δapg12* cells. Although significant amounts of Aut7p-PE were produced in these mutants (Figure 14), GFP-Aut7FGp did not localize to the pre-autophagosomal structure (Table II). This result indicates that the Apg12p-Apg5p conjugate is absolutely required for the proper localization of Aut7p. The role of the conjugate is not restricted to the localization of Aut7p, however, as *Δapg5* cells possess more severe defects in API maturation than the *Δaut7* cells (Abeliovich *et al.*, 1999; Abeliovich *et al.*, 2000).

Class C* apg *mutants do not recruit either Apg5p or Aut7p to the pre-autophagosomal structure

In class C mutants, *Δvps30*, *Δapg9*, *Δapg14* and *Δapg16*, neither Apg5p-GFP nor GFP-Aut7p localized to the pre-autophagosomal structure. *VPS30* and *APG14* are the genes involved in the autophagy-specific PI3-kinase complex. Double disruptant *Δapg1Δvps30* or *Δapg1Δapg9*, expressing GFP-Aut7p demonstrated a diffuse cytoplasmic staining pattern (Table II). This result indicates that *VPS30* and *APG9* (class C) are epistatic to *APG1* (class A) in the organization of the pre-autophagosomal structure. Therefore, the class C *APG* genes play roles in the organization of Apg5p and Aut7p on the pre-autophagosomal structure in a class A gene-independent manner. I further analyzed the levels of Aut7p-PE in these mutants. *Δapg16* cells contained significant levels of Aut7p-PE during vegetative growth (Figure 14A). The ratio of Aut7p-PE to unmodified Aut7p, however, decreased after nitrogen starvation (Figure 14B). The levels of Aut7p-PE in growing cells and starved cells were similar (data not shown), indicating that the synthesis of Aut7p during starvation resulted in a decrease in the relative levels of Aut7p-PE in *Δapg16* cells. In contrast, *Δvps30*, *Δapg9*, *Δapg14* cells possessed normal levels of Aut7p-PE, regardless of the nutrient conditions (Figure 14).

Apg16p is a coiled-coil protein linking the Apg12p-Apg5p conjugates (Mizushima *et al.*, 1999). Although the Apg12p-Apg5p conjugate was formed, I did not observe a dot structure of Apg5p-GFP in *Δapg16* cells (Table II). This observation suggests that the interaction of Apg5p and Apg16p is necessary for the proper localization of Apg5p to the pre-autophagosomal structure. Although Aut7p-PE was formed in the *Δapg16* mutant during vegetative growth (Figure 14A), I could not observe the localization of Aut7p to the pre-autophagosomal structure (Table II). This phenotype is similar to that of *Δaut2Δapg10* or *Δaut2Δapg12* cells expressing GFP-Aut7FGp (Table II), which contain significant levels of Aut7p-PE (Figure 15). This result indicates that Apg12p-Apg5p-Apg16p complex formation is needed for the localization of Aut7p. As *Δapg16* mutant failed to maintain Aut7p-PE levels during starvation, the Apg12p-Apg5p-Apg16p complex must be necessary for the maintenance of Aut7p-PE levels.

Two types of PI3-kinase complexes contain Vps34p, Vps15p and Vps30p/Apg6p as common components (Kihara *et al.*, 2001a). In these complexes, Apg14p and Vps38p are the components specifying autophagy or the carboxypeptidase Y (CPY), a vacuolar resident enzyme, sorting pathway, respectively. In *Δapg14* cells, Aut7p and Apg5p were located diffusely throughout the cytoplasm, whereas in *Δvps38* cells, the pre-autophagosomal

structure was detectable (Table II). In Δ*vps30* and Δ*apg14* strains, Aut7p-PE and the Apg12p-Apg5p conjugate were produced normally (Figure 14; Mizushima *et al.*, 1998). These results indicate that the autophagy-specific PI3-kinase complex is essential to recruit Aut7p-PE and the Apg12p-Apg5p conjugate to the pre-autophagosomal structure. The Δ*apg9* mutant also demonstrates class C phenotype. This fact suggests that Apg9p has a related function with the autophagy-specific PI3-kinase complex, although a physical interaction of Apg9p with other Apg proteins has not been identified.

Further genetic analysis based on the localization of GFP-Aut7p in* apg *mutants

As described in the above section, all *apg* mutants were categorized by the localization of GFP-Aut7p and Apg5p-GFP. I further investigated *apg* mutants during rapamycin-treated conditions. Under growing conditions, the pre-autophagosomal structure labeled with GFP-Aut7p was observed only in class A mutants; not in class B and C mutants (Figure 16A-D and Figure 9). The localizations did not alter in a few-hours treatment with rapamycin (data not shown). However, after the 24 h of the treatment, *apg* mutants showed distinct terminal phenotypes that correlate with the above classification (Figure 16). The class C mutants (Δ*apg16*, Δ*vps30*, Δ*apg9* and Δ*apg14*) could be further dissected based on their terminal phenotypes.

All class B mutants, including the Aut7 system and the Apg12 system, displayed the same phenotype. They contained only one dot in the cytosol after 24 h rapamycin treatment (Figure 16E). Since the dot was not always localized proximal to the vacuole, it may not correspond to the pre-autophagosomal structure. The terminal phenotypes of the class C mutants were divided into three. The phenotype of Δ*apg16* cells was indistinguishable from that of class B (class C1; Figure 16E). It is reasonable that the mutants of the Apg12 system and Δ*apg16* show the similar phenotype. Apg16p must be involved in the localization of Aut7p by interacting with the Apg12p-Apg5p conjugate. Δ*vps30* possessed multiple dots outside the vacuole (class C2; Figure 16F). Δ*apg9* and Δ*apg14* cells showed the same phenotype, that is, they contained a vacuole having a brightly stained rim (class C3; Figure 16G). Class A mutants were showed the essentially same phenotype. They contained multiple dots in the cytoplasm (Figure 16H).

Next, I examined the epistatic relations between class A, C1, C2, C3 and B by constructing inter-class double mutants. The phenotypes of double mutants exhibited simply either one phenotype of the single mutants (Table III). The class B mutants were epistatic to the other class C2, C3 and A mutants, the class C1 mutant was epistatic to the class C2 and

C3, the class C2 mutants were epistatic to the class C3 and A, and the class C3 was epistatic to the class A. Therefore, the order of epistasis was B, (C1), C2, C3 and A, which is consistent with the above classification. Terminal structures of the class B and C mutants may be dead-end structures but these structures may somehow reflect the Aut7p pathway to the pre-autophagosomal structure. Class C2 (*Δvps30*) was epistatic to class C3 (*Δapg9* and *Δapg14*). This difference is possibly caused by the remaining activity of PI3-kinase complex specific to the CPY pathway. When both *APG14* and *VPS38* are disrupted, both autophagy-specific PI3-kinase and CPY pathway-specific PI3-kinase lose their functions. As expected, *Δapg14Δvps38* double disruptant showed the same phenotype with *Δvps30* (Figure 16F). It was noteworthy that a portion of *Δapg2* (class A) cells showed the staining pattern of vacuolar rim. 42% cells contained such vacuoles (144 cells were counted), whereas 3% of *Δapg1* cells contained such vacuoles (130 cells were counted). I examined *Δapg1Δapg2* cells and found that this double disruptant displayed the phenotype of *Δapg1* (5% of cells showed the vacuolar rim pattern). *APG2* was hypostatic to the other *APG* genes. As a consequence of these analyses, I could dissect the process of Aut7p recruitment to the pre-autophagosomal structure. This analysis must provide important clues for investigating the itinerary of Aut7p.

Visualization of dynamics of cargo delivery mediated by autophagosomes

In the above sections, I followed the dynamics of autophagosome formation mainly by using GFP-Aut7p as a marker. In this section, I address the dynamics of API, one of the specific cargoes that are delivered to vacuoles via autophagosomes. Electron microscopic study has shown that the precursor API (proAPI) forms a large complex, namely the Cvt complex, which is enwrapped by Cvt vesicles or autophagosomes, then delivered to the vacuole (Baba *et al.*, 1997). Using API-GFP, I expected to analyze a molecular basis for the mechanism of general cargo delivery by autophagosomes.

I made a strain expressing carboxy-terminally GFP fused API by a direct integration method (Longtine *et al.*, 1998) and checked that API-GFP was correctly integrated by PCR analysis (data not shown). Immunoblot analysis indicated that proAPI-GFP was processed to become mature API (Figure 17, lane 7) and that GFP portion was cleaved on/after processing (Figure 17, lane 7). A small amount of mature API was detected in cells expressing proAPI-GFP under growing conditions (Figure 17, lane 3), indicating that proAPI-GFP is less effectively processed than proAPI. However, the amount of proAPI-GFP elevated by rapamycin treatment (Figure 17, lane 4 and 8) as seen in cells expressing proAPI (Figure 17, lane 2 and 6). This fact suggests that the expression of proAPI-GFP is regulated normally.

Integrating these facts, it is probable that proAPI-GFP is delivered to the vacuole through normal pathways. Under the fluorescence microscope, wild-type cells expressing API-GFP contained one or a few dots in the proximity to the vacuole and the slightly fluorescent vacuole in vegetative growth (Figure 18A-D). After rapamycin treatment, the fluorescence intensity in the vacuole increased but some cells possessed dots in the proximity to the vacuole (Figure 18E). In the *Δpep4* mutant, Cvt complexes are detected in autophagic bodies under nitrogen starvation conditions (Baba *et al.*, 1997). Therefore, I examined the localization of API-GFP in the *Δpep4* mutant. As expected, autophagic bodies were labeled with the fluorescence of API-GFP under rapamycin-treated conditions (data not shown). The above results show that API-GFP is a useful marker to trace the dynamics of cargoes delivered by autophagosomes. Furthermore, I found that Cvt complexes are detectable by fluorescence microscopy with API-GFP. The complex is localized close to the vacuole like the pre-autophagosomal structure, and transported to the vacuole via autophagosome.

I examined whether the Cvt complex was localized on the pre-autophagosomal structure by immunofluorescence microscopy with anti-Aut7p antibody. Aut7p was essentially colocalized with the complex (Figure 19), showing that the Cvt complex was localized on the pre-autophagosomal structure. Next, I checked the formation of the Cvt complex in *apg* mutants (*Δapg1*, *Δvps30/Δapg6*, *Δapg9*, *Δapg14* and *Δapg16*). API-GFP was not delivered to the vacuolar lumen during growing and starvation conditions. Instead, the Cvt complex remained outside the vacuole as one bright dot (Figure 20). I showed that the formation of the Cvt complex was not impaired in the above *apg* mutants. Other factors may be involved in the organization of the complex.

Cvt19p, a receptor that is essential for the cytoplasm-to-vacuole targeting (Cvt) pathway, is one of the candidates for such a factor. Cvt19p is localized near the vacuole as a dot and delivered to the vacuole through the Cvt and Apg pathways (Scott *et al.*, 2001). *Δcvt19* cells show severe defects in the maturation of API under growing and rapamycin-treated conditions and proAPI binding to the membrane is destabilized in *Δcvt19* cells (Scott *et al.*, 2001). Therefore, I observed whether Cvt19p is involved in the organization of the Cvt complex using *Δcvt19* cells. Cvt complexes were normally detected but brighter than those in wild type cells (Figure 21). In rapamycin-treated cells, the fluorescence got brighter but the lumen of the vacuoles was not stained (data not shown). These results suggest that in the *Δcvt19* cells, the organization of the Cvt complex is normal but its delivery to the vacuole is severely impaired. Since bulk protein degradation progresses normally in this mutant (Scott *et*

al., 2001), the Δ*cvt19* cell may have a defect in targeting the Cvt complex to the autophagosomal membrane; not in the formation of autophagosomes.

To examine the dynamics of the Cvt complex delivery to the vacuole, API-GFP was observed in *apg1*^{ts} cells under the fluorescence microscope. I performed a time-lapsed examination after temperature shift-down from 37°C to 30°C. Just after temperature decrease, the Cvt complex remained outside the vacuole as a bright dot (Figure 22A, 45 min and B, 14 min) like Δ*apg1* cells (Figure 20). In 20 minutes after the transition to 30°C, the complex entered the vacuole (24 min, N = 18) and the fluorescence of API-GFP rapidly diffused throughout the vacuolar lumen in following one minute (74 sec, N = 17; Figure 22A, 75 sec and B, 37 sec), indicating that autophagic bodies were disintegrated by vacuolar hydrolases immediately after entering the vacuole. This observation suggested that API-GFP, accumulated in the Cvt complex by incubating at 37°C, was transported to the vacuole by one or a small number of autophagosomes.

I constructed a strain expressing API-GFP and visualized that API gathers to the pre-autophagosomal structure as Cvt complexes in an *APG* genes-independent manner and the complex enters the vacuole via autophagy. By using API-GFP as a cargo marker, I will further investigate the relationship between autophagosome, cargo, and the pre-autophagosomal structure.

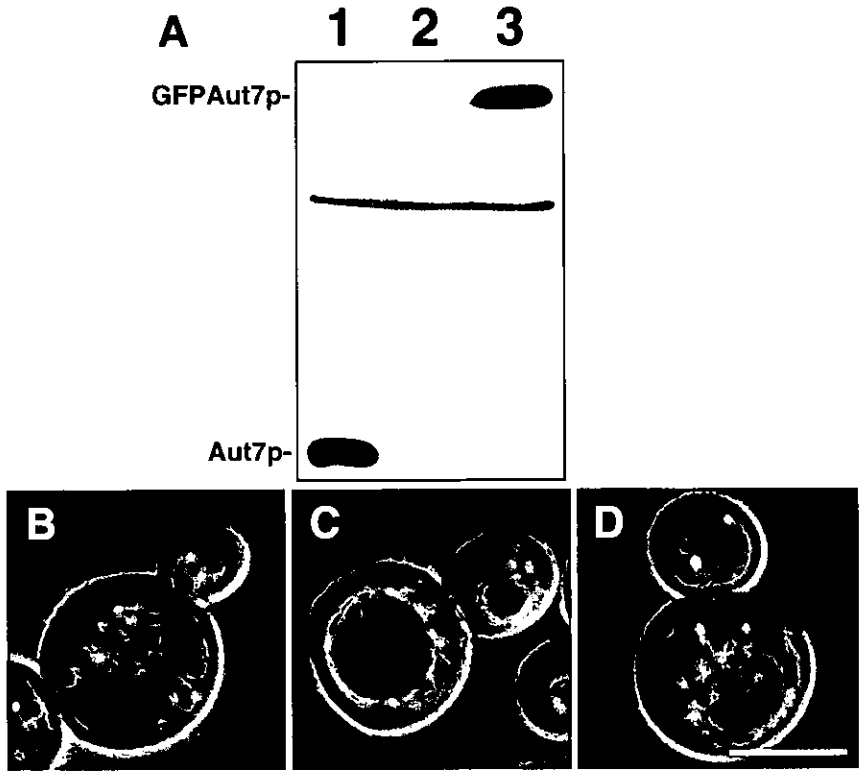

Figure 2. Functional GFP-Aut7p is expressed from a natural promoter at a physiological level. (A) The expression level of GFP-Aut7p under growing conditions. Cell lysates were prepared as described in Materials and methods. (1) Wild-type (KA311A), (2) Δ*aut7* (YYK218) and (3)Δ*aut7* (YYK218) expressing GFP-Aut7p. (B-D) The accumulation of autophagic bodies was examined under a light microscope. Cells were incubated for 6 h in 0.17 % yeast nitrogen base without amino acid and ammonium sulfate containing 1 mM PMSF. Nomarski images of (B) wild-type (KA311A), (C) Δ*aut7* (YYK218), (D) Δ*aut7* (YYK218) expressing GFP-Aut7p, Bar: 5 μm.

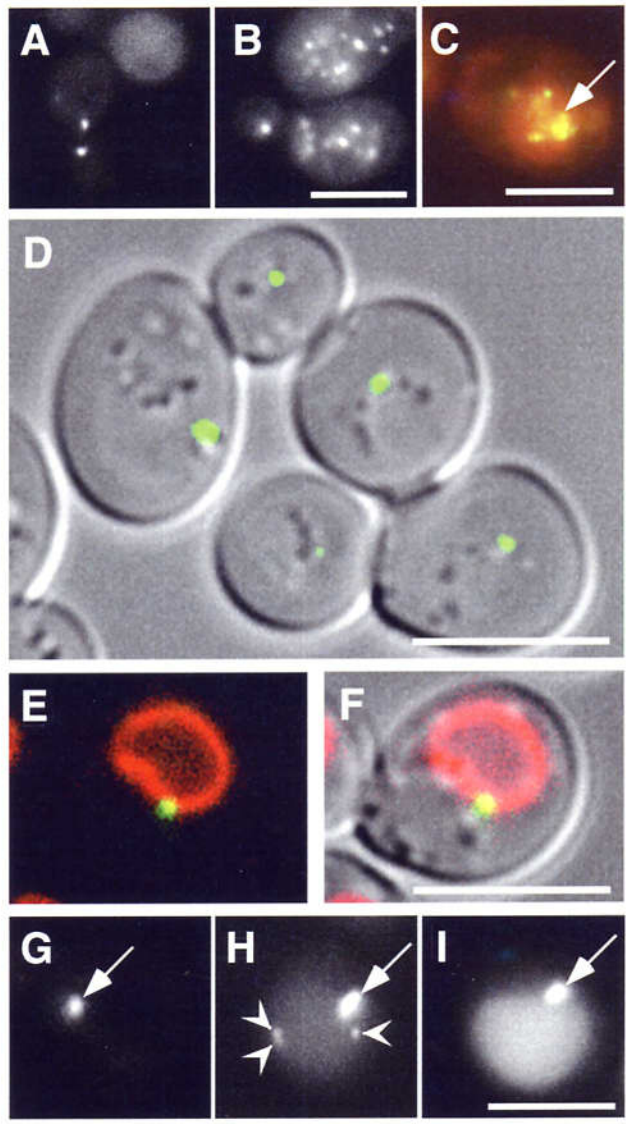

Figure 3. Localization of GFP-Aut7p. Cells expressing GFP-Aut7p were grown in SD + CA medium. (A and B) GFP-Aut7p in the Δ*ypt7* cell (KVY4). (A) A single punctate structure was detected during the vegetative growth. (B) Autophagosomes accumulated after 3 h rapamycin treatment. (C) GFP-Aut7p in a Δ*pep4*Δaut7 cell (KVY6) after 4 h treatment with rapamycin. Autophagic bodies were labeled with GFP-Aut7p in the vacuole (arrow). Merged image of GFP-Aut7p (green) and the vacuole labeled with FM4-64 (red). (D) GFP-Aut7p in the Δ*aut7* cell (KVY5) under growing conditions. The Nomarski image is overlaid with the fluorescence of GFP-Aut7p. One punctate structure per cell was detected during vegetative growth. (E and F) GFP-Aut7p in the Δ*aut7* cell (KVY5) under growing conditions. A punctate structure of GFP-Aut7p is detected close to the vacuole labeled with FM4-64. (E) Fluorescence of GFP-Aut7p (green) and a vacuole labeled with FM4-64 (red). (F) The Nomarski image is overlaid with the fluorescence of GFP-Aut7p and FM4-64. (G-H) GFP-Aut7p in a Δ*aut7* cell (KVY5). Punctate structures were detected close to the vacuole regardless of rapamycin treatment (arrows). (G) A cell under vegetative growth conditions. The punctate structures close to the vacuole were detected in 43 cells out of 206 cells (21%). (H) Additional dots (arrowheads) appeared in the cytosol after 1 h rapamycin treatment. (I) The cell after 5 h rapamycin treatment. Bar: 5 μm.

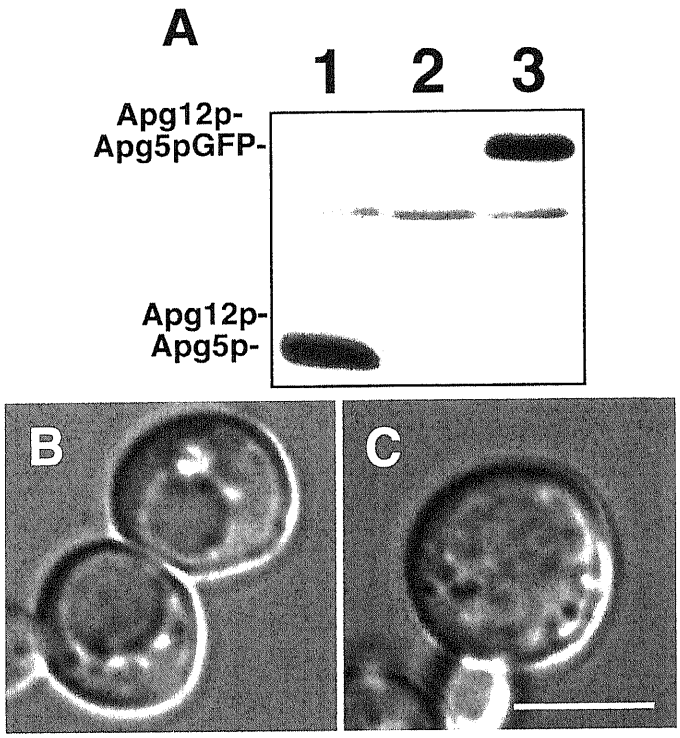

Figure 4. Functional Apg5p-GFP is expressed from a natural promoter at a physiological level. (A) The Apg12p-Apg5p conjugate was produced normally in Δ*apg5* cells expressing Apg5p-GFP. Cell lysates were prepared as described in Materials and methods. (1) Wild-type (KA311A), (2) Δ*apg5* (GYS59) and (3) Δ*apg5* (GYS59) expressing Apg5p-GFP. (B and C) The accumulation of autophagic bodies was examined under a light microscope. Cells were incubated for 6 h in 0.17 % yeast nitrogen base without amino acid and ammonium sulfate containing 1 mM PMSF. Nomarski images of (B) Δ*apg5* (GYS59) and (C) Δ*apg5* (GYS59) expressing Apg5p-GFP. Bar: 5 μm.

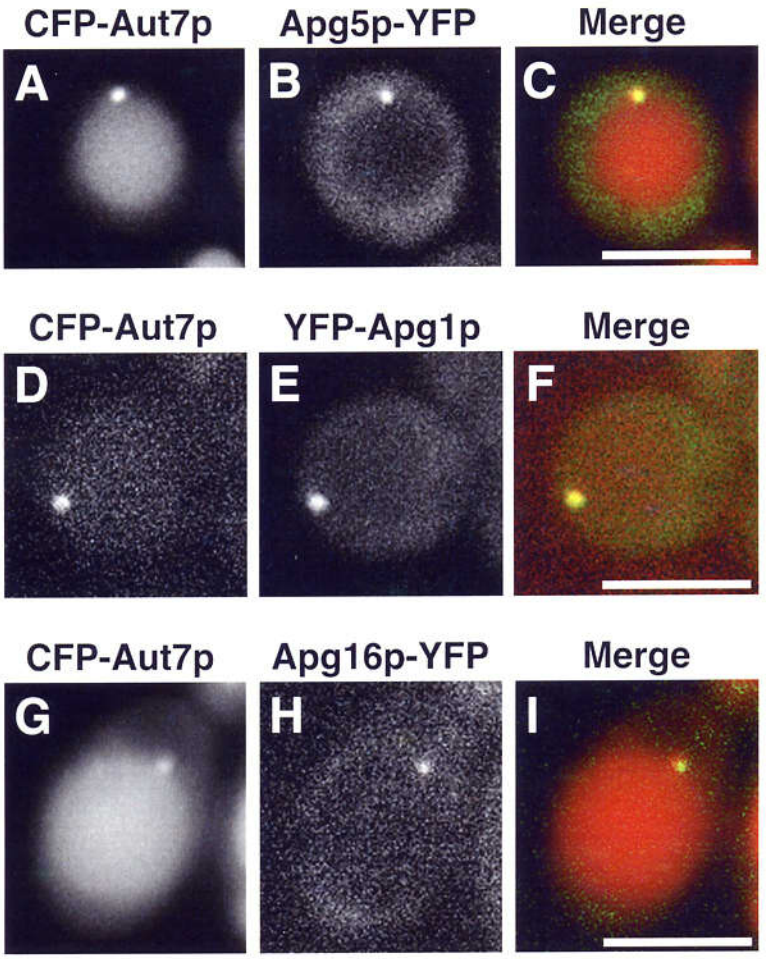

Figure 5. Colocalization of Apg1p, Apg5p, Apg16p and Aut7p on a punctate structure close to the vacuole. (A-C) Δ*apg5* cells (YNM119) expressing Apg5p-YFP and CFP-Aut7p were treated with rapamycin for 3 h. (A) Apg5p-YFP. (B) CFP-Aut7p. (C) Merged image of Apg5p-YFP (green) and CFP-Aut7p (red). (D-F) Δ*apg1* cells (NNY20) expressing CFP-Aut7p and YFP-Apg1p were treated with rapamycin for 30 min. (D) CFP-Aut7p. (E) YFP-Apg1p. (F) Merged image of CFP-Aut7p (red) and YFP-Apg1p (green). (G-I) Δ*apg16* cells (KVY117) expressing CFP-Aut7p and YFP-Apg16p were treated with rapamycin for 6 h. (G) CFP-Aut7p. (H) YFP-Apg16p. (I) Merged image of CFP-Aut7p (red) and YFP-Apg16p (green). Bar: 5 μm.

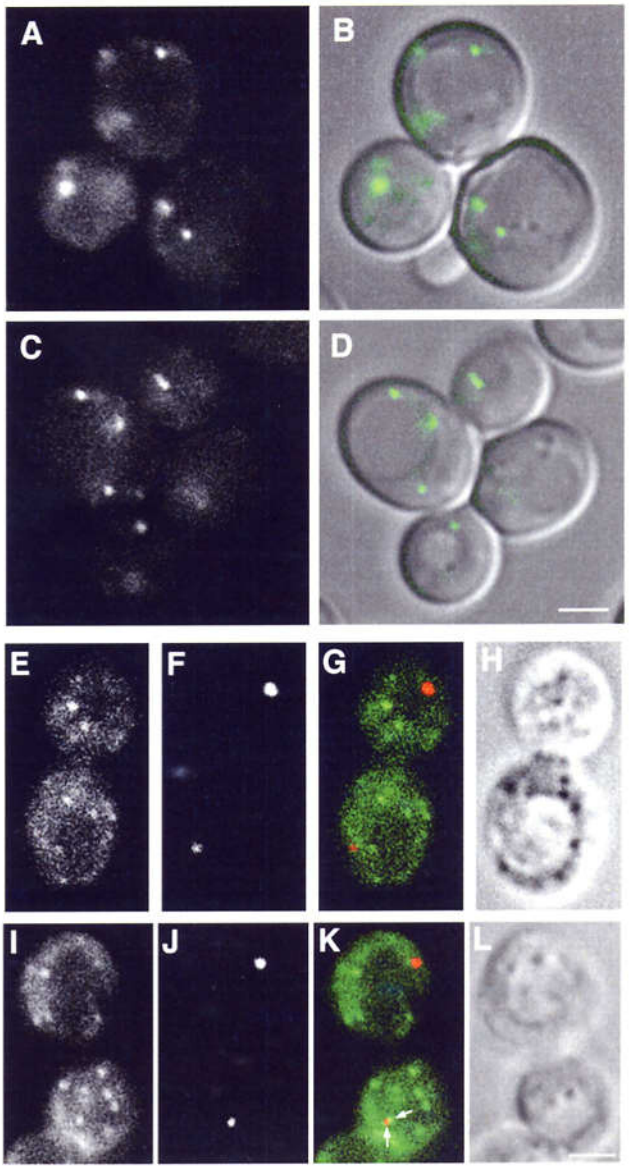

Figure 6. Localization of Aut7p and Apg9p-GFP. (A-B) Apg9p-GFP was visualized in Δ*apg9* cells (CTD1) under growing conditions. (A) Apg9p-GFP (B) The Nomarski image is overlaid with the fluorescence of Apg9p-GFP. (C-D) Apg9p-GFP in Δ*apg9*Δapg14 cells (GYS29) was identified under growing conditions. (C) Apg9p-GFP. (D) The Nomarski image is overlaid with the fluorescence of Apg9p-GFP. (E-L) Δ*apg9* cells (CTD1) expressing Apg9p-GFP were treated with rapamycin for 2 h. Immunofluorescence microscopy was performed as described in Materials and methods. (E and I) Apg9p-GFP. (F and J) Aut7p. (G and K) Merged images of Apg9p-GFP (green) and Aut7p (red). (H and L) Nomarski images. Apg9p and Aut7p were occasionally found in close proximity (arrows in K). Bar: 2 μm.

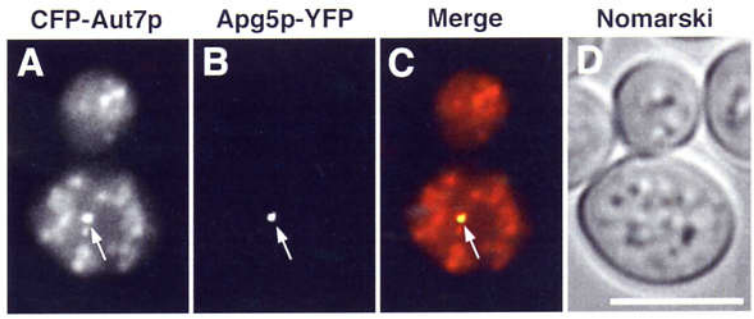

Figure 7. Localization of Aut7p and Apg5p in Δ*ypt7* cells. A Δ*ypt7*Δapg5 cell (YAK3) expressing CFP-Aut7p and Apg5p-YFP were treated with rapamycin for 5 h. (A) Autophagosomes stained with CFP-Aut7p. (B) Apg5p-YFP. (C) Merged image of CFP-Aut7p (red) and Apg5p-YFP (green). (D) Nomarski image. CFP-Aut7p and Apg5p-YFP colocalized on a punctate structure (arrows). Bar: 5 μm.

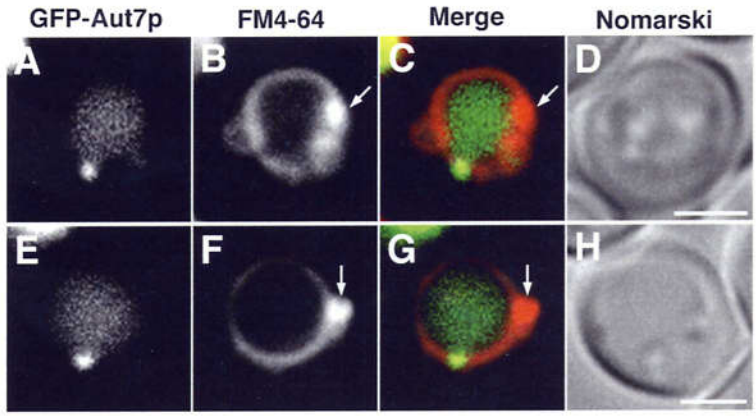

Figure 8. Localization of Aut7p and the class E compartment. The class E compartment of Δ*vps4* cells (MBY3) expressing GFP-Aut7p was labeled with FM4-64 as described in Materials and methods, following treatment with rapamycin for 2 h. (A and E) GFP-Aut7p. (B and F) The class E compartments stained with FM4-64 (arrows). (C and G) Merged images of GFP-Aut7p (green) and FM4-64 (red). (D and H) Nomarski images. Bar: 2 μm.

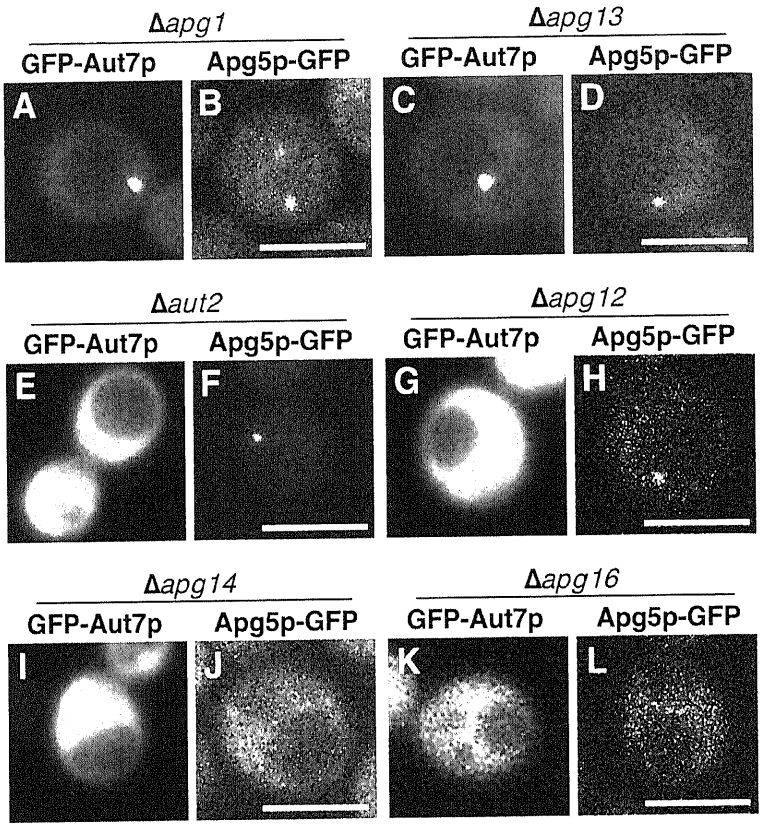

Figure 9. Localization of GFP-Aut7p and Apg5p-GFP in the *apg* mutants grown in SD + CA medium. (A) Δ*apg1* cells (NNY20). GFP-Aut7p was detected on a punctate structure close to the vacuole in 30 of 161 cells (18 %). Δ*apg13* (C; TFD13W2), Δ*apg17* (YYK111), *apg2* (MT2-4-4) cells exhibited an identical phenotype. (B) Δ*apg1* cells (YYK36) expressing Apg5p-GFP. Punctate structures were detected in 11 of 91 cells (12 %). Δ*apg13* (D; TFD13W2), Δ*apg17* (YYK111) and *apg2* (MT2-4-4) cells demonstrated an identical phenotype. (E) This image of a Δ*aut2* cell (GYS6) expressing GFP-Aut7p is representative of the Aut7 system. The punctate structures were detected in one of 78 cells (1 %). Δ*apg7* (GYS9) and Δ*aut1* (GYS5) cells exhibited the same phenotype. (F) Δ*aut2* cells (GYS6) expressing Apg5p-GFP. A single punctate structure was detected in 11 of 52 cells (21 %). Δ*aut1* (GYS5) and Δ*aut7* (YYK218) cells demonstrated a similar phenotype. (G) This Δ*apg12* cell (GYS13) expressing GFP-Aut7p is representative of mutants of the Apg12 system. Punctate structures were detected in one of 84 cells (1 %). Δ*apg10* (TFD10-L1) and Δ*apg5* (SKD5-1D) cells possessed an identical phenotype. (H) A Δ*apg5*Δapg12 cell (YNM117) expressing Apg5p-GFP. A single punctate structure was detected in 16 of 104 cells (15 %). Δ*apg7* (GYS9), Δ*apg10* (TFD10-L1) and Δ*apg5* (SKD5-1D) cells all exhibited an identical phenotype. (I) A Δ*apg14* cell (SKD14-1C) expressing GFP-Aut7p. None of the 51 cells displayed a punctate structure. Δ*vps30* cells (SKD6-1D) and Δ*apg9* cells (CTD1) possessed an identical phenotype. (J) A Δ*apg14* cell (AKY12) expressing Apg5p-GFP under growing conditions. Punctate structures were observed in one of 248 cells (less than 1 %). Δ*vps30* cells (AKY74) and Δ*apg9* cells (CTD1) exhibited an identical phenotype. (K) A Δ*apg16* cell (KVY117) expressing GFP-Aut7p. No punctate structures were observed in any of the 77 cells. (L) A Δ*apg5*Δapg16 cell (YNM126) expressing Apg5p-GFP under growing conditions. No punctate structures were observed in the 184 cells examined. Bar: 5 μm.

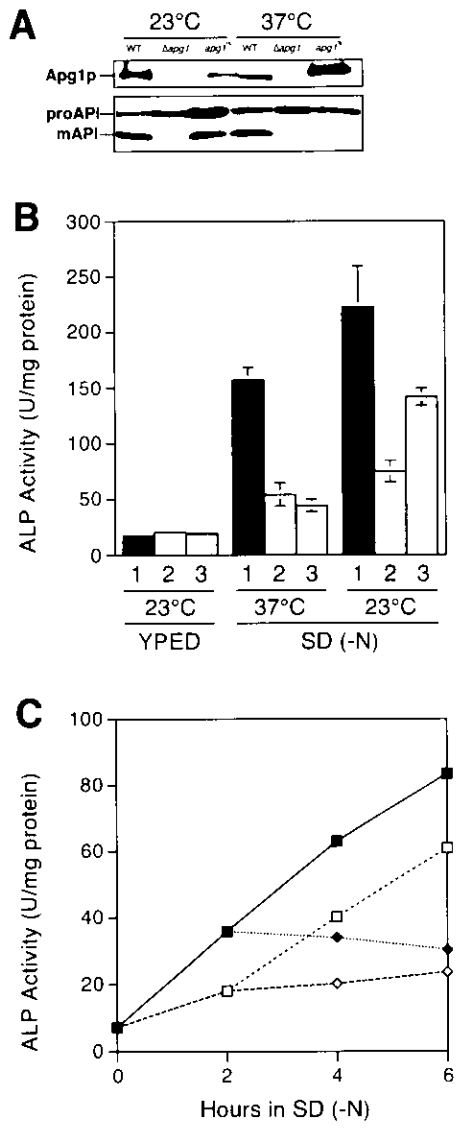

Figure 10. *apg1*^{ts} mutant possessing functional temperature sensitivity. (A) Although temperature sensitive Apg1p was detectable, the maturation of API was completely blocked at 37°C in *apg1*^{ts} cells. The API proform (proAPI) is processed to the mature API (mAPI) in an Apg1p activity-dependent manner. Wild-type cells (TN125), Δ*apg1* cells (YYK126) and Δ*apg1* cells (YYK126) carrying the apg1^{ts} plasmid were grown in YEPD medium at 23°C or 37°C overnight. Apg1p and API were detected as described in Materials and methods. (B) Δ*apg1* cells (YYK126) carrying (1) the APG1 plasmid, (2) the vector or (3) the apg1^{ts} plasmid were grown in YEPD medium at 23°C. They were then transferred into SD (-N) medium at 23°C or 37°C and incubated for 6 h before ALP activity was measured. (C) Δ*apg1* cells (YYK126) carrying the apg1ts plasmid were grown in YEPD medium at 23°C. The cells were then transferred into SD (-N) medium and incubated at 23°C or 37°C. (closed squares) Cells starved continuously at 23°C. (open squares) Cells incubated for 2 h at 23°C and then transferred to 37°C. (open lozenges) Cells starved continuously at 37°C. (closed lozenges) Cells incubated for 2 h at 37°C and then transferred to 23°C.

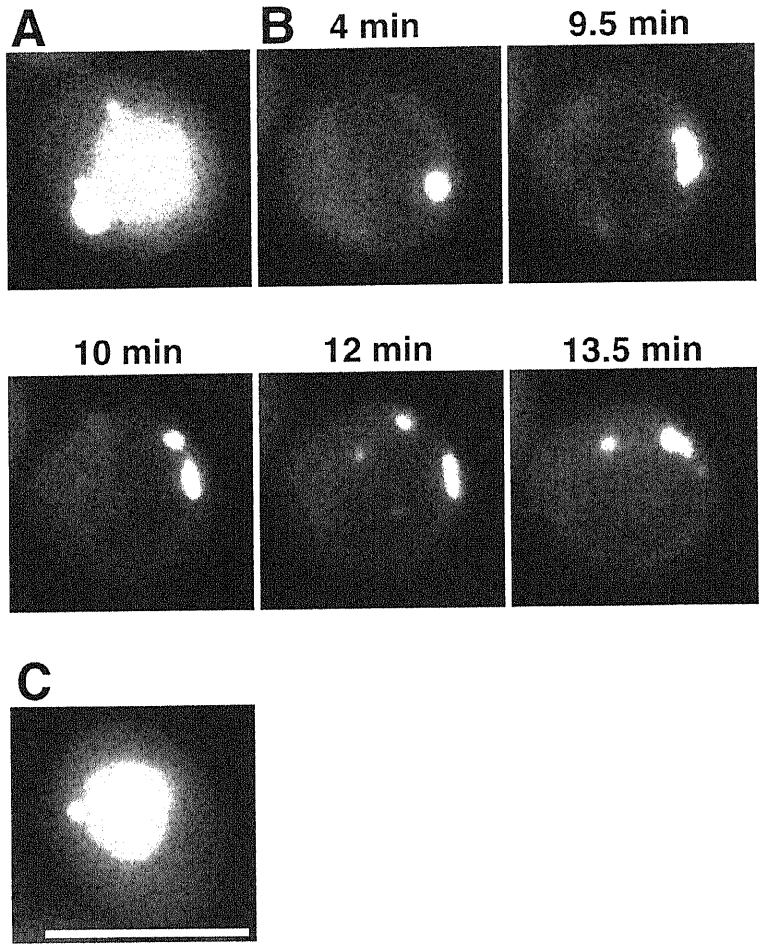

Figure 11. Time-lapsed microscopy of *apg1*^{ts} cells expressing GFP-Aut7p. Δ*apg1* cells (NNY20) carrying the apg1ts and GFP-Aut7p plasmids were used. (A) Cells treated with rapamycin for 3 h at 30°C. (B) Time-lapse images following temperature decrease. Cells were treated with rapamycin for 4 h at 37°C before decreasing the temperature to 30°C. (C) Cells incubated for 2 h at 30°C after temperature decrease. Bar: 5 μm.

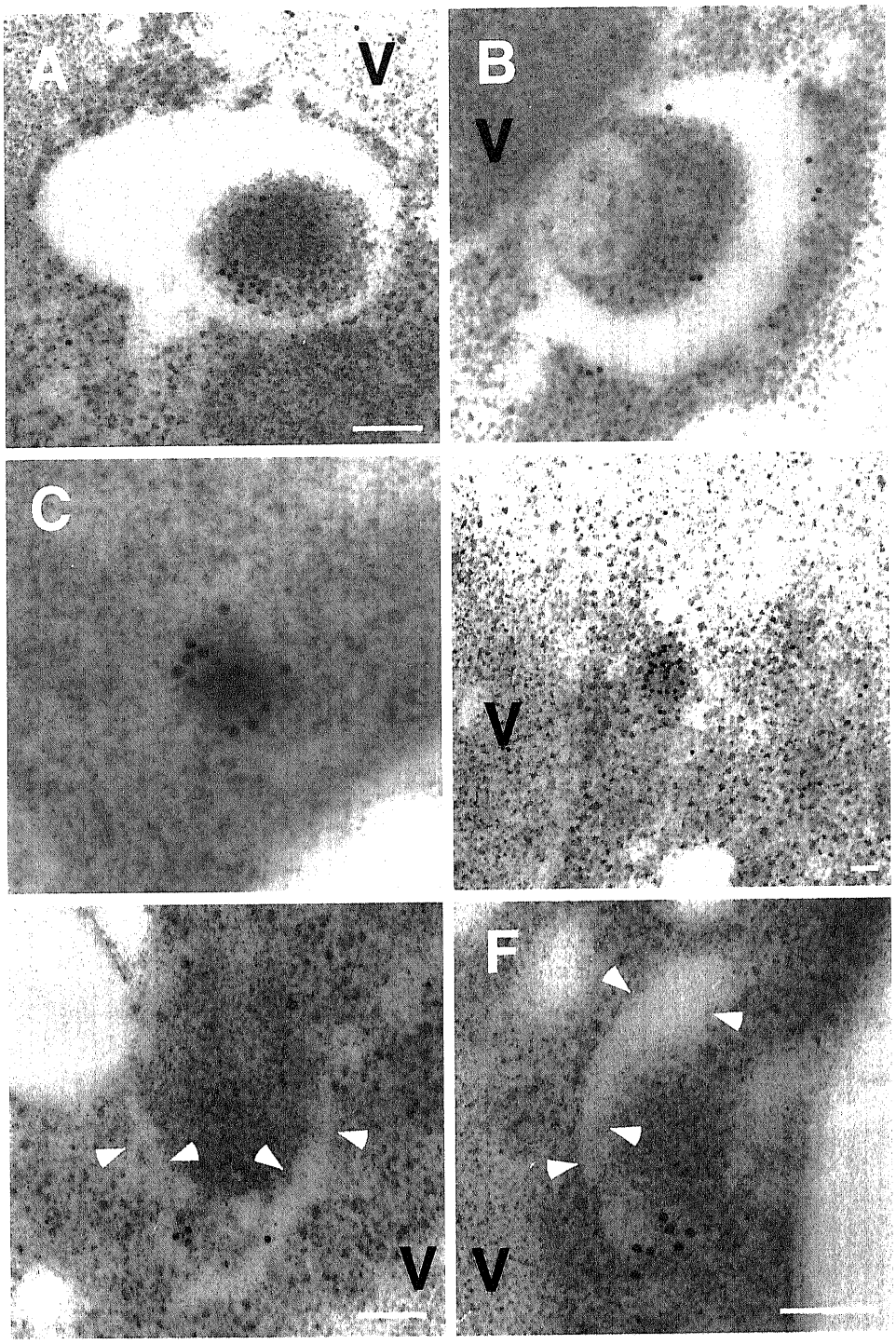

Figure 12. Localization of Aut7p and Apg2p by immunoelectron microscopy. Δ*aut7* cells (KVY5) expressing HA-Aut7p were treated with rapamycin for 6 h. Thin sections were immunolabeled with anti-HA antibody (A-C) or anti-Apg2p antibody (D-F). V: Vacuoles. Arrowheads in E and F: circular isolation membranes. Bar: 100 nm (A, B, E and F) and 50 nm (C and D)

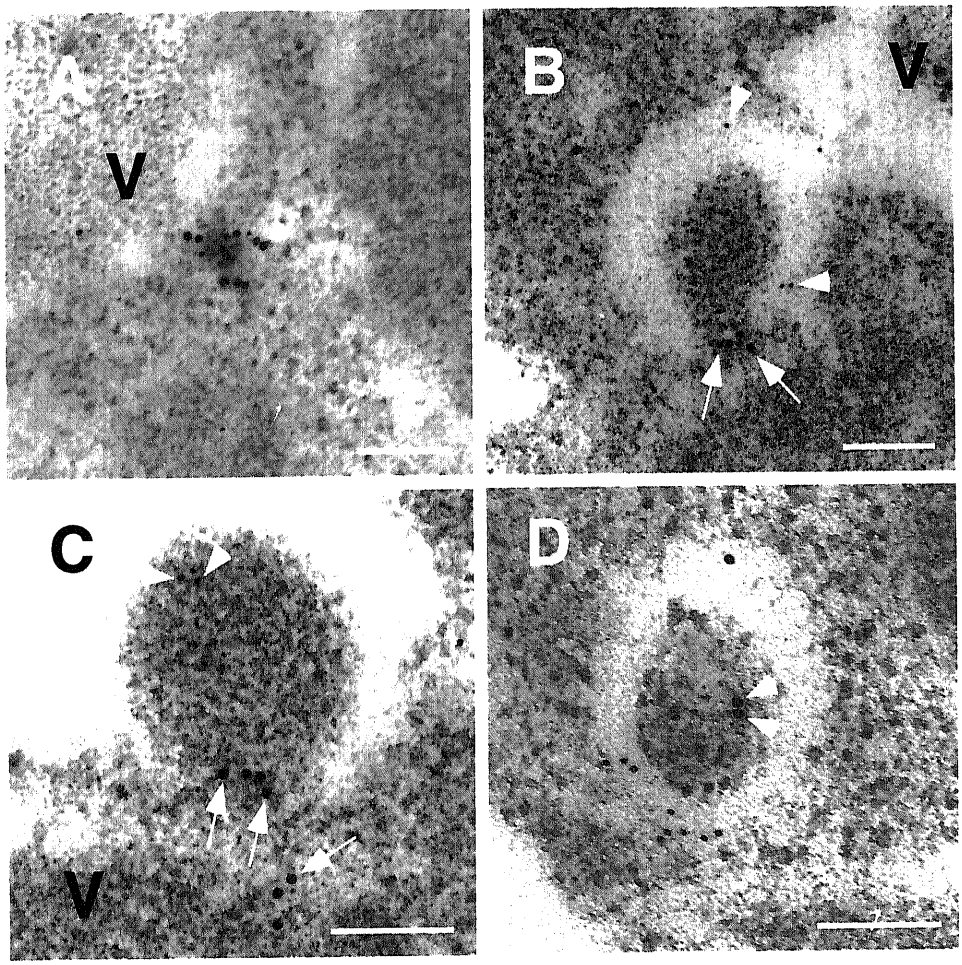

Figure 13. Localization of Aut7p and Apg2p by double-labeling. Δ*aut7* cells (KVY5) expressing HA-Aut7p were treated with rapamycin for 6 h. Thin sections were immunolabeled with mixture of anti-HA antibody and anti-Apg2p antibody. (A and D) Aut7p (larger particles) and Apg2p (smaller particles). (B and C) Aut7p (smaller particles) and Apg2p (larger particles). V: Vacuoles. Arrowheads: Aut7p. Arrows: Apg2p. Bar: 100 nm.

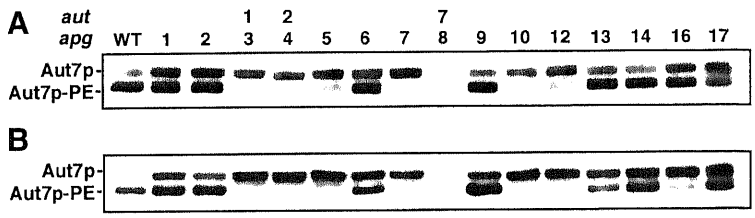

Figure 14. Levels of Aut7p-PE present in each *apg* mutant. Lysates were prepared by glass beads disruption prior to SDS-PAGE as described in Materials and methods. (A) Cells in vegetative growth. (B) Cells following a 4.5 h starvation in SD (-N) medium. We examined the phenotype of wild-type (SEY6210), Δ*apg1* (GYS102), *apg2* (MT2-4-4), Δ*aut1* (KVY113), Δ*aut2* (KVY13), Δ*apg5* (KVY142), Δ*vps30* (KVY135), Δ*apg7* (KVY118), Δ*aut7* (KVY5), Δ*apg9* (KVY114), Δ*apg10* (KVY136), Δ*apg12* (KVY115), Δ*apg13* (KVY116), Δ*apg14* (GYS115), Δ*apg16* (KVY117) and Δ*apg17* (YYK111) cells.

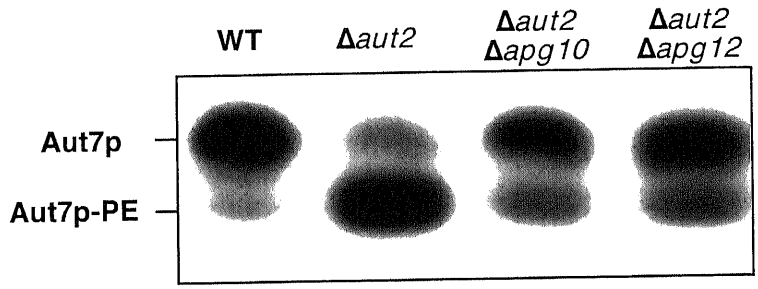

Figure 15. Amounts of Aut7p-PE in Δ*aut2* cells expressing Aut7FGp during vegetative growth. Lysates were prepared by glass beads disruption and subjected to SDS-PAGE as described in Materials and methods. The strains used in this experiment are as follows: wild-type (SEY6210), Δ*aut2* (KVY13), Δ*aut2*Δ*apg10* (KVY150) and Δ*aut2*Δ*apg12* (KVY148).

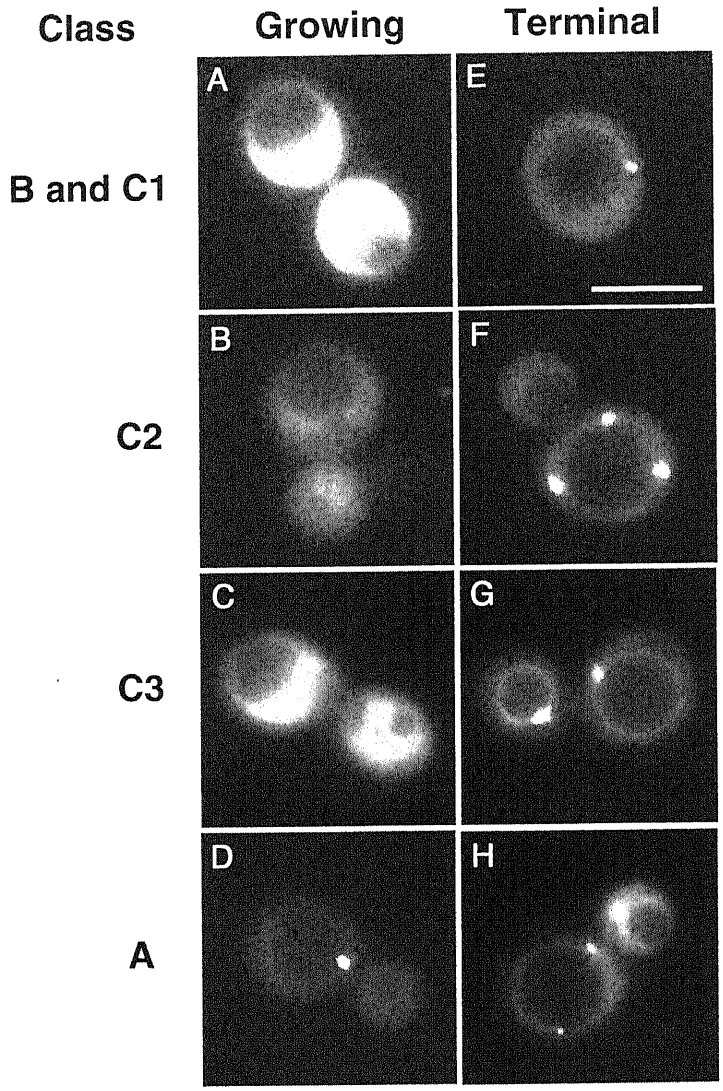

Figure 16. Localization of GFP-Aut7p in *apg* mutants after 24 h-rapamycin treatment. Cells expressing GFP-Aut7p were grown in SD + CA medium and observed under the fluorescence microscope. (A and E) Δ*aut2* cells (GYS6) showing the class B phenotype. (B and F) Δ*vps30* cells (SKD6-1D) showing the class C2 phenotype. (C and G) Δ*apg9* cells (CTD1) showing the class C3 phenotype. (D and H) Δ*apg1* cells (NNY20) showing the class A phenotype, (A-D) Cells before rapamycin treatment and (E-H) after 24 h-rapamycin treatment. Bar: 5 μm.

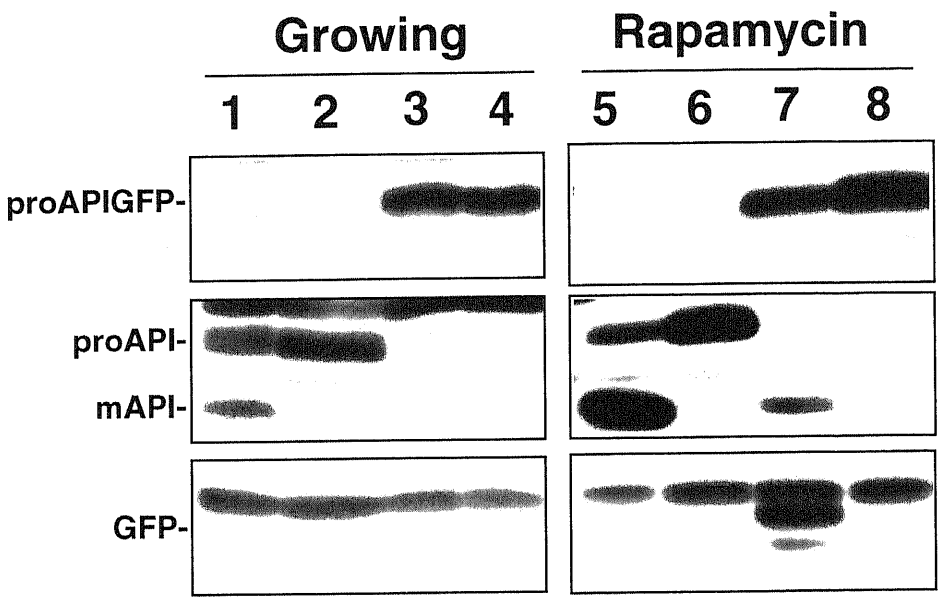

Figure 17. Processing of API-GFP. Cell lysates were prepared as described in Materials and methods. (1 and 5) Wild-type cells (SEY6210), (2 and 6) Δ*apg1* cells (GYS102), (3 and 7) wild-type cells expressing API-GFP (GYS244), (4 and 8) Δ*apg1* cells expressing API-GFP (GYS237). (1-4) Cells grown in YEPD medium. (5-8) Cells treated with rapamysin for 3 h.

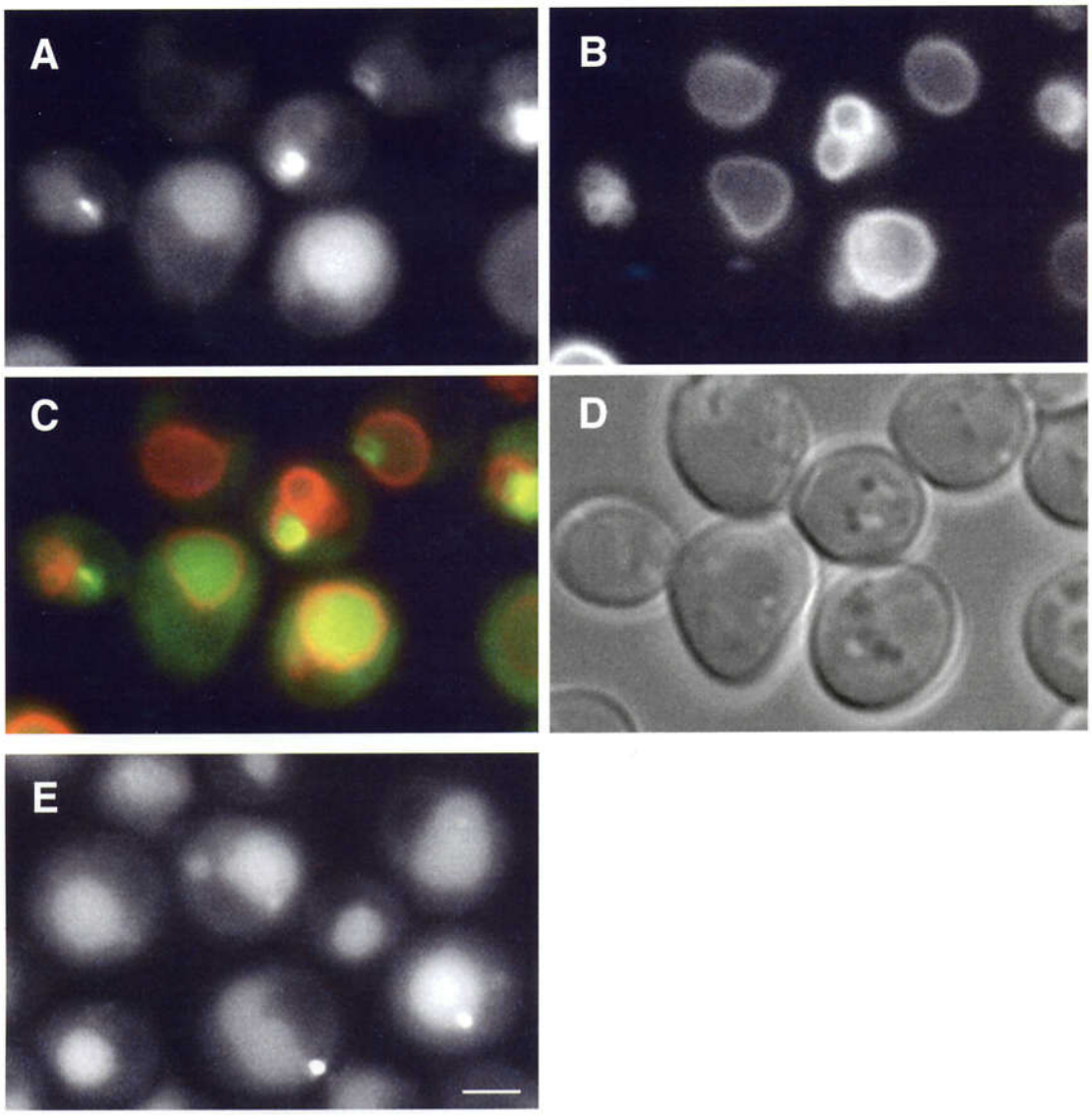

Figure 18. Localization of API-GFP. (A-D) Wild-type cells expressing API-GFP (GYS244) under growing conditions and (E) after 4 h-rapamycin treatment. (A and E) API-GFP, (B) vacuoles labeled with FM4-64, (C) merged image, and (D) Nomarski image. Bar: 2μm.

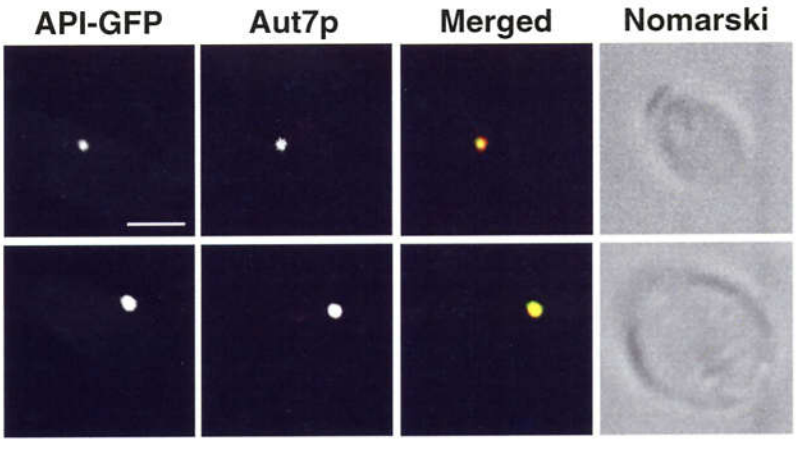

Figure 19. Colocalization of API-GFP and Aut7p on the pre-autophagosomal structure. Wild-type cells expresing API-GFP (GYS244) were treated with rapamycin for 3 h and fixed with formaldehyde. Aut7p was visualized by immunofluorescence microscopy as described in Materials and methods. Bar: 2µm.

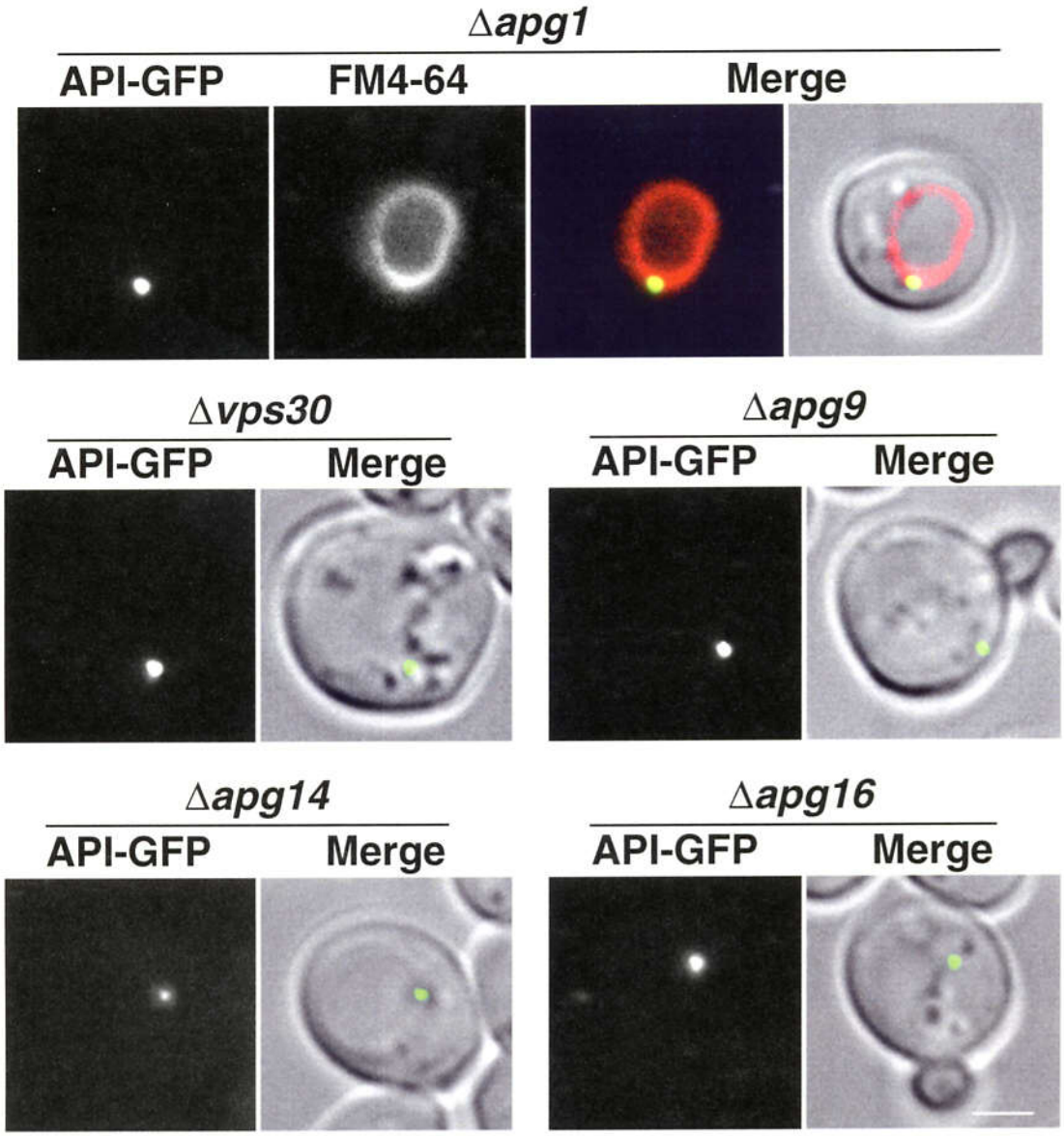

Figure 20. Localization of API-GFP in *apg* mutants. Δ*vps30* (GYS249), Δ*apg9* (GYS252), Δ*apg14* (GYS255) and Δ*apg16* (GYS257) cells expressing API-GFP were grown in SD + CA medium. Δ*apg1* cells (GYS237) were treated with rapamycin for 3 h. The vacuolar membrane of Δ*apg1* cells was stained with FM4-64. Bar: 2μm.

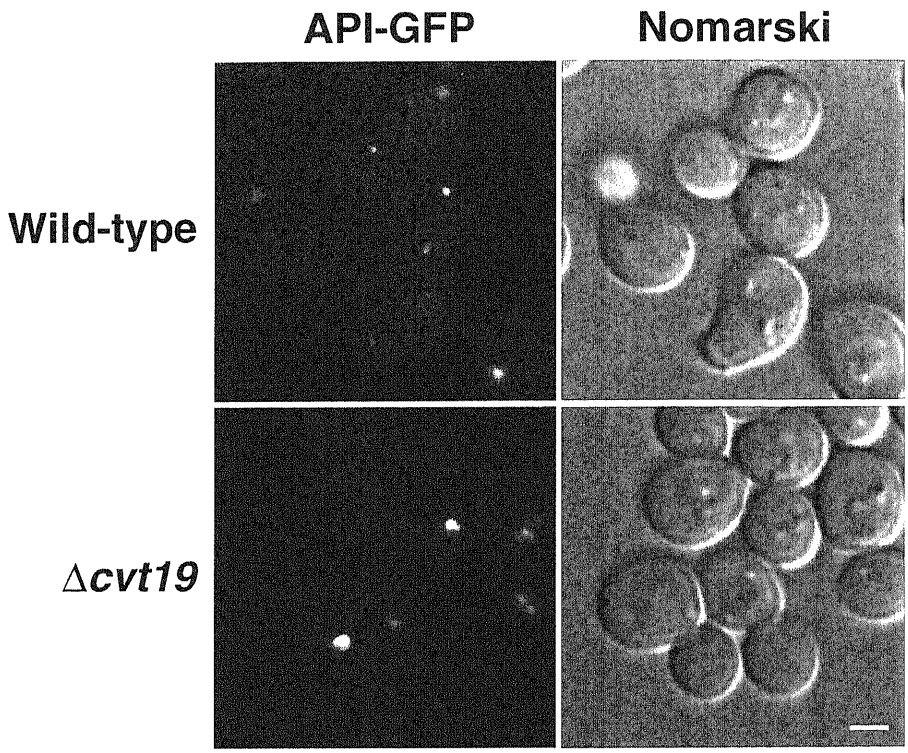

Figure 21. Localization of API-GFP in wild-type (GYS244) and Δ*cvt19* (GYS286) cells. Cells were grown in SD + CA medium. Bar: 2μm.

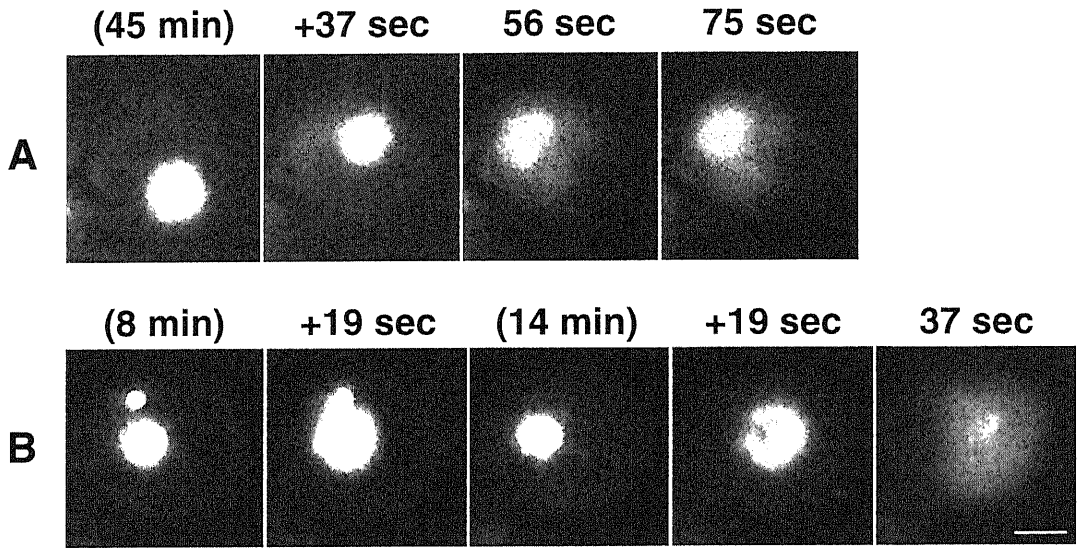

Figure 22. Time-lapse microscopy of *apg1*^{ts} cells expressing API-GFP. Δ*apg1* cells (GYS237) carrying the apg1^{ts} plasmid were treated with rapamycin for 3 h at the non-permissive temperature. Images were acquired after temperature decrease to the permissive temperature. Numbers in parentheses indicate the time after temperature decrease. Bar: 2μm.

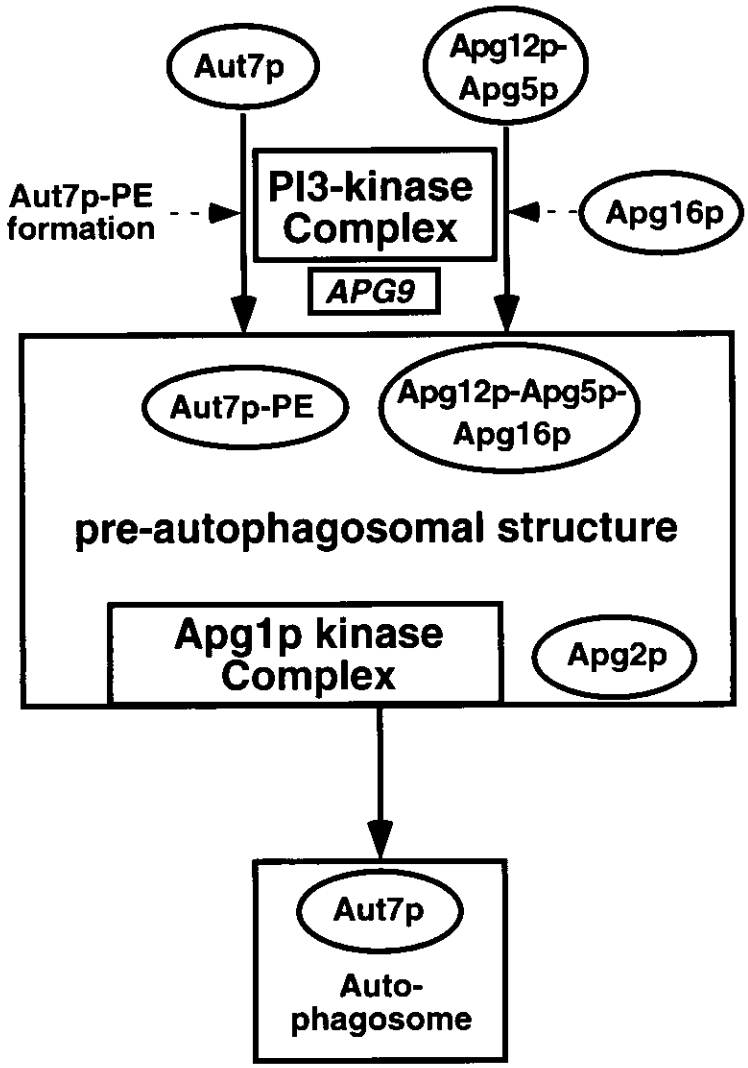

Figure 23. Proposed model for the concerted interaction of Apg proteins. Aut7p, the Apg12p-Apg5p-Apg16p complex and the Apg1p kinase complex function on the pre-autophagosomal structure. The localization of Aut7p and the Apg12p-Apg5p-Apg16p on the pre-autophagosomal structure depends on the action of the autophagy-specific PI3-kinase complex and Apg9p. The Apg1p kinase complex is directly involved in the formation of autophagosomes. See the text for details.

Table I. Strains Used in this Study

Strain	Genotype	Source
SEY6210	*MATα ura3 leu2 his3 trp1 lys2 suc2*	Darsow *et al.*, 1997
YW5-1B	*MAT***a** *ura3 leu2 trp1*	Tsukada and Ohsumi, 1993
KA311A	*MAT***a** *ura3 leu2 his3 trp1*	K. Irie (Osaka University, Japan)
KA311B	*MATα ura3 leu2 his3 trp1*	K. Irie (Osaka University, Japan)
BJ2168	*MAT***a** *ura3 leu2 trp1 pep4-3 prb1-1122 prc1-407*	Yeast Genetic Stock Center
TN125	*MAT***a** *ade2 ura3 leu2 his3 trp1 lys2 pho8::pho8Δ60*	Noda and Ohsumi, 1998
GYS102	SEY6210 *Δapg1::LEU2*	This study
MT2-4-4	*MATα leu2 ura3 apg2*	Tsukada and Ohsumi, 1993
KVY113	SEY6210 *Δaut1::LEU2*	This study
KVY13	SEY6210 *Δaut2::LEU2*	Kirisako *et al.*, 2000
KVY142	SEY6210 *Δapg5::LEU2*	This study
KVY135	SEY6210 *Δvps30::LEU2*	Kirisako *et al.*, 2000
KVY118	SEY6210 *Δapg7::HIS3*	Kirisako *et al.*, 2000
KVY5	SEY6210 *Δaut7::HIS3*	Kirisako *et al.*, 1999
KVY114	SEY6210 *Δapg9::TRP1*	This study
KVY136	SEY6210 *Δapg10::HIS3*	This study
KVY115	SEY6210 *Δapg12::HIS3*	This study
KVY116	SEY6210 *Δapg13::TRP1*	This study
GYS115	SEY6210 *Δapg14::LEU2*	This study
KVY117	SEY6210 *Δapg16::LEU2*	This study
NNY20	YW5-1B *Δapg1::LEU2*	Matsuura *et al.*, 1997
GYS5	YW5-1B *Δaut1::TRP1*	Ichimura *et al.*, 2000
GYS6	YW5-1B *Δaut2::LEU2*	Ichimura *et al.*, 2000
SKD5-1D	YW5-1B *Δapg5::LEU2*	Kametaka *et al.*, 1996
SKD6-1D	YW5-1B *Δvps30::LEU2*	Kametaka *et al.*, 1998
GYS9	YW5-1B *Δapg7::LEU2*	Ichimura *et al.*, 2000
CTD1	YW5-1B *Δapg9::TRP1*	Noda *et al.*, 2000
TFD10-L1	YW5-1B *Δapg10::LEU2*	Shintani *et al.*, 1999
GYS13	YW5-1B *Δapg12::TRP1*	This study
TFD13W2	YW5-1B *Δapg13::TRP1*	Funakoshi *et al.*, 1997
SKD14-1C	YW5-1B *Δapg14::LEU2*	Kametaka *et al.*, 1998
YYK36	KA311A *Δapg1::LEU2*	Kamada *et al.*, 2000
GYS59	KA311A *Δapg5::HIS3*	This study
YNM119	KA311B *Δapg5::HIS3*	Mizushima *et al.*, 1998
AKY74	KA311A *Δvps30::LEU2*	This study
YYK218	KA311A *Δaut7::TRP1*	This study
AKY12	KA311A *Δapg14::LEU2*	This study
YYK111	KA311A *Δapg17::HIS3*	Kamada *et al.*, 2000
YYK190	BJ2168 *Δapg1::LEU2*	This study

YYK126	TN125 *Δapg1::LEU2*	Kamada *et al.*, 2000
YAK3	SEY6210 *Δypt7::HIS3 Δapg5::LEU2*	This study
MBY3	SEY6210 *Δvps4::TRP1*	Babst *et al.*, 1997
YNM117	*MAT***a** *ura3 leu2 trp1 Δapg5::LEU2 Δapg12::HIS3*	Mizushima *et al.*, 1999
YNM126	KA311B *Δapg5::HIS3 Δapg16::LEU2*	Mizushima *et al.*, 1998
GYS21	YW5-1B *Δvps30::LEU2 Δapg12::TRP1*	This study
GYS22	KA311A *Δapg1::LEU2 Δapg7::HIS3*	This study
GYS23	YW5-1B *Δapg1::URA3 Δvps30::LEU2*	This study
GYS24	YW5-1B *Δapg1::LEU2 Δapg9::TRP1*	This study
GYS25	YW5-1B *Δvps30::LEU2 Δapg9::TRP1*	This study
GYS26	*MAT***a** *ura3 apg5 Δvps30::LEU2*	This study
GYS27	YW5-1B *Δaut1::LEU2 Δapg9::TRP1*	This study
GYS29	YW5-1B *Δapg9::TRP1 Δapg14::LEU2*	This study
GYS33	YW5-1B *Δapg5::LEU2 Δapg14::TRP1*	This study
GYS35	SEY6210 *Δvps30::LEU2 Δapg16::LEU2*	This study
GYS37	SEY6210 *Δapg9::TRP1 Δapg16::LEU2*	This study
GYS64	YW5-1B *Δapg1::URA3 Δapg2::LEU2*	This study
KVY150	SEY6210 *Δaut2::LEU2 Δapg10::HIS3*	This study
KVY148	SEY6210 *Δaut2::LEU2 Δapg12::HIS3*	This study
GYS244	SEY6210 *API::API-GFP-KAN*	This study
GYS237	SEY6210 *API::API-GFP-KAN Δapg1::LEU2*	This study
GYS249	SEY6210 *API::API-GFP-KAN Δvps30::LEU2*	This study
GYS252	SEY6211 *ADE2 API::API-GFP-KAN Δapg9::TRP1*	This study
GYS255	SEY6210 *API::API-GFP-KAN Δapg14::LEU2*	This study
GYS257	SEY6210 *API::API-GFP-KAN Δapg16::LEU2*	This study
GYS286	SEY6210 *API::API-GFP-KAN Δcvt19::LEU2*	This study
GYS259	SEY6210 *API::API-GFP-KAN Δpep4::LEU2*	This study

Table II. Localization of GFP-Aut7p and Apg5p-GFP on the punctate structure in *apg* mutants

Genotype	GFP-Aut7p	Apg5p-GFP
Δapg1	+	+
apg2	+	+
Δaut1/Δapg3	-	+
Δaut2/Δapg4	-	+
Δapg5	-	+ (WT)
Δvps30/Δapg6	-	-
Δapg7	-	+
Δaut7/Δapg8	+ (WT)	+
Δapg9	-	-
Δapg10	-	+
Δapg12	-	+
Δapg13	+	+
Δapg14	-	-
Δapg16	-	-
Δapg17	+	+
Δapg1Δapg7	-	not examined
Δapg1Δvps30	-	not examined
Δapg1Δapg9	-	not examined
Δaut2Δapg10	-	not examined
expressing GFP-Aut7FGp		
Δaut2Δapg12	-	not examined
expressing GFP-Aut7FGp		
Δvps38	+	not examined

+: GFP-Aut7p or Apg5p-GFP is localized to the punctate structure.

-: GFP-Aut7p or Apg5p-GFP shows a diffuse cytoplasmic staining pattern.

WT: wild-type.

Table III. Classification of *apg* double mutants based on the localization of GFP-Aut7p

	A	B (C1)	C2	C3
A		B (*Δapg1 Δapg7*)	C2 (*Δapg1 Δvps30*)	C3 (*Δapg1 Δapg9*)
B (C1)			B (*apg5Δvps30*, *Δvps30Δapg12*, *Δvps30Δapg16*)	B (*Δaut1Δapg9*, *Δapg5Δapg14*, *Δapg9Δapg16*)
C2				C2 (*Δvps30 Δapg9*)
C3				

Cells expressing GFP-Aut7p were observed under the fluorescence microscope. Samples were taken after 24 h of rapamycin treatment and their phenotypes were checked. Strains used in this experiment were as follows: *Δapg1Δapg7* (GYS22), *Δapg1Δvps30* (GYS23), *Δapg1Δapg9* (GYS24), *apg5Δvps30* (GYS26), *Δvps30Δapg12* (GYS21), *Δvps30Δapg16* (GYS35), *Δaut1Δapg9* (GYS27), *Δapg5Δapg14* (GYS33), *Δapg9Δapg16* (GYS37) and *Δvps30Δapg9* (GYS25).

Discussion

In this study, I systematically investigated the localization of GFP-tagged Apg proteins when expressed at physiological levels. This analysis identified a novel punctate structure close to the vacuole, namely "pre-autophagosomal structure", in which Apg1p, Apg2p, Apg5p, Aut7p and Apg16p are assembled (Figure 23). Apg5p and Aut7p are recruited to the structure by the action of Apg16p and the autophagy-specific PI3-kinase complex. The Apg1p protein kinase complex is also localized to the structure. This kinase functions in concert with the Apg12p-Apg5p-Apg16p complex and Aut7p to play a crucial role in generating autophagosomes. My characterization of this structure uncovered that Apg proteins exist in three functional groups, the Apg1p protein kinase complex, the ubiquitin-like systems (the Apg12 system and the Aut7 system) and the autophagy-specific PI3-kinase complex. Epistatic analyses of the *apg* mutant phenotypes clearly uncovered the interrelationship on the pre-autophagosomal structure between these three groups. Although the functions of the *APG2* and *APG9* genes remain unknown, I obtained results suggesting that these genes encode proteins acting close to the Apg1p protein kinase complex and the autophagy-specific PI3-kinase complex, respectively.

The pre-autophagosomal structure

Following rapamycin treatment, the fluorescence of GFP-Aut7p and other GFP-fused Apg proteins visualizing the pre-autophagosomal structure rapidly increase in intensity (data not shown). The amount of Aut7p increases during autophagy, whereas there is no significant increase of Apg1p, Apg2p, Apg5p or Apg16p during autophagy. These results suggest the further recruitment of Apg proteins to the pre-autophagosomal structure by unknown mechanisms. This change in the composition of the pre-autophagosomal structure may initiate autophagosome formation.

Repeated cell fractionation analyses of Apg proteins have not uncovered a biochemical identification of the pre-autophagosomal fraction. It is likely that low levels of each Apg protein are recruited onto the structure; in addition, the structure may be unstable in cell lysates, leading to difficulties in its biochemical characterization. Aut7p is concentrated on circular isolation membranes (Figures 12B and 13B) and Aut7p-enriched regions near the vacuole (Figures 12C and 13A), as determined by immunoelectron microscopy (Kirisako *et al.*, 1999). This Aut7p-enriched region is one candidate for the pre-autophagosomal structure. The intensive examination of Aut7p-concentrated structures, however, did not yet succeed in

identifying a definite membrane structure corresponding to the pre-autophagosomal structure. Recently, the analyses based on fluorescence microscopy, suggested that Apg2p is a specific marker for the pre-autophagosomal structure (Shintani *et al.*, 2001). By immunoelectron microscopy with an anti-Apg2p antibody, I demonstrated that Apg2p was localized near Aut7p, but showed distinct patterns from Aut7p during autophagosome formation (Figure 13B-D). Apg2p was concentrated on a membrane-like structure next to the circular isolation membrane labeled with Aut7p, suggesting that Apg2p and Aut7p have different roles in autophagosome formation. In *Δapg2* cells, Aut7p and the Apg12p-Apg5p conjugate normally recruited onto the pre-autophagosomal structure (Figure 9 and Table II) but cannot generate autophagosomes in the absence of Apg2p. This fact indicates that Apg2p is involved in the formation of autophagosomes on the pre-autophagosomal structure. My observation by immunoelectron microscopy also showed that Apg2p was not localized on the isolation membrane or the lumen of autophagosomes. Apg2p may have roles in extending membranes of autophagosomes from the pre-autophagosomal structure. Currently, it is still unclear whether the pre-autophagosomal structure is membranous. Further analyses are essential for determining the structure where Apg2p localizes.

I demonstrated the dynamics of autophagosome generation involving the pre-autophagosomal structure. Experiments using the *apg1*^{ts} strain indicated that autophagosomes labeled with GFP-Aut7p separated from the pre-autophagosomal structure after shifting to the permissive temperature (Figure 11B), then entered the vacuole (Figure 11C). This result suggests that the pre-autophagosomal structure is an organizing center for autophagosomes. Each dot corresponds to the pre-autophagosomal structure or an autophagosome; currently, it is difficult to distinguish autophagosomes from the pre-autophagosomal structure by solely observing GFP-Aut7p. This *apg1*^{ts} strain is useful to collect autophagosomes in the course of formation. I expect to identify the detailed ultrastructure of the pre-autophagosomal structure by careful examination of the open region of circular isolation membranes.

The organization of the pre-autophagosomal structure is not affected in the class A mutants, *Δapg1*, *Δapg2*, *Δapg13* or *Δapg17*. Furthermore, I demonstrated that Apg1p is a component of the pre-autophagosomal structure (Figure 5D-F). Apg13p and Apg17p are also likely components of the structure, as Apg1p interacts directly with Apg13p and Apg17p (Kamada *et al.*, 2000). In response to nutrient depletion, enhanced activity of the Apg1p kinase complex controls switching from Cvt vesicle formation under growing conditions to autophagosome formation under starvation conditions. Aut7p is normally induced in *Δapg1* cells by rapamycin or starvation (Kirisako *et al.*, 1999). Therefore, the Apg1p kinase complex

plays a role both in autophagy signaling and autophagosome formation. The delivery of GFP-Apg1p to the vacuolar lumen during rapamycin treatment (data not shown) also supports the involvement of Apg1p in the latter stage of autophagosome formation.

Organization of the pre-autophagosomal structure

Aut7p-PE is a component of the pre-autophagosomal structure (Figure 9 and Table II). I demonstrated that the absence of the Apg12p-Apg5p conjugate results in a severe decrease in Aut7p-PE levels (Figure 14). Aut7p-PE is not localized on the pre-autophagosomal structure in *Δaut2Δapg10*, *Δaut2Δapg12* cells (Table II). These data suggest that the Apg12p-Apg5p conjugate must play a role in the localization of Aut7p-PE in addition to the generation of Aut7p-PE. Upon rapamycin treatment, however, *Δaut7* cells show some degree of API maturation, whereas *Δapg5* cells contain no mature API (Abeliovich *et al.*, 1999; Abeliovich *et al.*, 2000; Kirisako *et al.*, 2000). This suggests that the Apg12p-Apg5p conjugate is essential for both autophagosome formation and the localization of Aut7p-PE on the pre-autophagosomal structure.

Apg16p forms a complex with the Apg12p-Apg5p conjugate (Mizushima *et al.*, 1999). GFP-Aut7p exhibits a diffuse staining pattern in *Δapg16* cells, regardless of the normal levels of Aut7p-PE present during vegetative growth (Figure 14A). *Δapg16* mutant failed to increase the level of Aut7p-PE during starvation (Figure 14B). Apg16p may participate in the maintenance of the Aut7p-PE levels during starvation. Apg5p-GFP also possesses a diffuse pattern throughout the cytosol in *Δapg16* cells (Figure 9L). The localization of Apg16p to the structure (Figure 5G-I) suggests that Apg16p plays a role in targeting the Apg12p-Apg5p conjugate to the pre-autophagosomal structure. In *Δapg16* cells, Aut7p-PE may not be localized on the pre-autophagosomal structure due to a lack of the Apg12p-Apg5p-Apg16p complex.

I did not observe GFP-Aut7p punctate structures in growing *Δapg9* cells (Table II); the punctate structures are reported in *Δapg9* cells under nitrogen-starved conditions (Kim *et al.*, 2001). To investigate the localization of GFP-Aut7p during autophagy, I examined GFP-Aut7p in rapamycin-treated *Δapg9* cells. I observed a similar punctate staining pattern similar to that described by Kim *et al.* (data not shown; Kim *et al.*, 2001). These punctate structures, however, were less distinct and of a lower intensity than those seen in *Δapg1* cells (data not shown). This result suggests that Apg9p plays an important role in the recruitment of Aut7p to the pre-autophagosomal structure.

The autophagy-specific PI3-kinase complex controls the organization of the pre-autophagosomal structure, but the PI3-kinase complex specific to the CPY pathway does not. In autophagy-specific PI3-kinase complex mutants, both Aut7p-PE and the Apg12p-Apg5p conjugate are produced normally, indicating that these conjugation reactions occur in the absence of the complex. It is a plausible hypothesis that Aut7p-PE and the Apg12p-Apg5p are transported to the pre-autophagosomal structure via vesicles. One possible function of the autophagy-specific PI3-kinase complex is to select cargo during vesicle budding (Kihara *et al.*, 2001a). The complex may load Aut7p-PE and/or the Apg12p-Apg5p conjugate into vesicles to facilitate their transport to the pre-autophagosomal structure. A second possibility is that the complex plays a role in vesicular sorting, allowing those containing Aut7p-PE and/or the Apg12p-Apg5p conjugate to be delivered to the pre-autophagosomal structure. There is also a third possibility that the PI3-kinase complex provides the pre-autophagosomal structure with phosphatidylinositol 3-phosphate (PI3P); PI3P then mediates the localization of the Apg12p-Apg5p conjugate and Aut7p-PE to the structure. Analysis of the autophagy-specific PI3-kinase during the organization of the pre-autophagosomal structure will further the understanding of general membrane dynamics mediated by PI3-kinases.

Terminal phenotypes based on the localization of Aut7p during autophagy

Since the class B phenotype was epistatic to the other phenotypes, it is likely that the lipidation of Aut7p is required for the proper localization of Aut7p on the pre-autophagosomal structure. However, the lipidation itself was not enough for the localization, because the pre-autophagosomal structure was not observed in class C mutants during vegetative growth in spite of significant amount of Aut7p-PE (Figure 14). The mislocalization of Apg5p-GFP in class C mutants suggests that the proper localization of the Apg12p-Apg5p conjugate is required for the localization of Aut7p on the pre-autophagosomal structure. The class C phenotypes were epistatic to the class A. It was unexpected that *Δvps30/Δapg6* (class C2) and *Δapg14* (class C3) showed different terminal phenotypes (Figure 16F and G), since they form a protein complex (Kametaka *et al.*, 1998). In addition, it was reported that Vps30p is a component of two distinct PI3-kinase complexes: one is the autophagy-specific PI3-kinase complex, which consists of Vps34p-Vps15p-Vps30p-Apg14p and the other is the CPY pathway-specific PI3-kinase complex, which consists of Vps34p-Vps15p-Vps30p-Vps38p. *Δvps30* cells lack both complexes, but *Δapg14* cells are defective only in the autophagy-specific PI3-kinase complex. *Δvps34* cells showed a terminal phenotype similar to that of the *Δvps30* cells (data not shown). This result suggests

that the terminal phenotype of Δ*vps30* (Figure 16F) is probably caused by the defect in both kinase complexes. The terminal phenotype of Δ*apg14* cells (Figure 16G) is possibly caused by the remaining activity of the CPY pathway-specific PI3-kinase complex. This hypothesis was supported by the observation that the Δ*apg14*Δ*vps38* double disruptant, which was defective in both complexes, also showed the Δ*vps30* phenotype, not Δ*apg14* phenotype (data not shown). In the Δ*apg14* cell, Aut7p could be transported to the vacuolar membrane in the presence of *VPS38* function. This phenomenon may correlate with the previous observation that a mutated plasma membrane ATPase, Pma1p, which is mislocalized to the vacuole, becomes localized in the plasma membrane in the absence of Vps38p (Luo and Chang, 1997). These results suggest that lack of the PI3-kinase activity leads to the phenotype of the class C2 or C3. *APG9* also belongs to the class C3. Apg9p is a putative membrane protein required for autophagy (Noda *et al.*, 2000). The phenotype of Δ*apg9* is the same with that of Δ*apg14*. This fact suggests that Apg9p and Apg14p function in a close or identical step of autophagy.

In the absence of Aut2p, Aut7p-PE accumulates in a membrane fraction (Kirisako *et al.*, 2000). In fact, Δ*aut2*Δ*apg9* cells expressing GFP-Aut7FGp, the terminal phenotype, the vacuolar membrane staining pattern, became prominent even in growing conditions (data not shown). This result suggests that the terminal structures in class C mutants are a consequence of the accumulation of Aut7p-PE. There are two possible interpretations for the class C2 phenotype. First, the structures in Δ*vps30* cells represent the intermediates delivering Aut7p to the pre-autophagosomal structure in a *VPS30* and *VPS34*, the PI3-kinase, dependent manner. This model proposes that Aut7p is transported to the pre-autophagosomal structure through this intermediate structure. Second, Aut7p is mislocalized to non-physiological terminal structures due to lack of *VPS30* or *VPS34* function. In either case, the class C2 and C3 genes are necessary for the proper localization of Aut7p on the punctate structure. Apg5p was not localized on the punctate structure in the class C2 and C3 mutants, either. This defect is not caused by the mislocalization of Aut7p, because Apg5p is normally localized in Δ*aut7* cells. Membrane dynamics mediated by PI3-kinase should be important for the organization of the pre-autophagosomal structure.

The class A genes, which consist of the Apg1p kinase complex (*APG1*, *APG13* and *APG17*) and *APG2*, were hypostatic to the class B and C genes. The organization of the pre-autophagosomal structure is not affected by the class A mutations (Table II and Figure 9A and B). The experiment using *apg1*^{ts} cells demonstrated that the class A genes are involved in the process of autophagosome formation after the pre-autophagosomal structure was organized (Figure 11). The phenotype of *apg2* during growing conditions suggests that

Apg2p is involved in a close step to the Apg1p kinase complex. However, the kinase activity of Apg1p is not impaired by an *apg2* mutation (Kamada, personal communication), suggesting that Apg2p is not a regulatory factor of Apg1p. The localization of Apg2p to the pre-autophagosomal structure does not depend on the kinase activity of Apg1p but on the existence of Apg1p (Shintani *et al.*, 2001). In contrast, Apg1p localizes normally to the pre-autophagosomal structure in the absence of Apg2p (data not shown). The terminal phenotype of Δ*apg2* based on the localization of GFP-Aut7p was slightly different from that of Δ*apg1* and hypostatic to Δ*apg1* (data not shown). Moreover, Apg1p was delivered to the vacuole during autophagy (Figure 5E) but Apg2p was not (Shintani *et al.*, 2001). These facts indicate that Apg1p and Apg2p have closely related but distinct roles for autophagosome formation.

Delivery of cargos of autophagosomes

To dissect the processes of delivery of contents of autophagosomes, I constructed a strain that expresses API-GFP under the control of the natural promoter. API-GFP seems to be transported to the vacuole through normal pathways: API-GFP is delivered into the vacuole under growing conditions (Figure 18A-D) and the amount of API-GFP increases by rapamycin-treatment (Figure 17). ProAPI is known to form a dodecamer using its N-terminal pro-region (Kim *et al.*, 1997), to bind membranes to become pelletable (Kim *et al.*, 1997), and to form large complexes that are detectable by electron microscopy, i.e. Cvt complexes. The complexes are directly enwrapped by autophagosomes or Cvt vesicles, and delivered to the vacuole. In this study, I found that Cvt complexes are observable with API-GFP by fluorescence microscopy. The temperature-shift experiments clarified that Cvt complexes labeled with API-GFP are delivered to the vacuole depending on the *apg1*^{ts} activity (Figure 22). By examining *apg1*^{ts} cells under an electron microscope, I will judge whether the dot of API-GFP is actually the Cvt complex. In the *apg1*^{ts} cells, accumulated API-GFP by incubating at the non-permissive temperature is transported to the vacuole via one autophagosome and degraded by the action of vacuolar hydrolases (Figure 22). It takes approximately 20 min API-GFP to enter the vacuole after temperature decrease, suggesting the sum of the time of autophagosome formation and autophagosome fusion to the vacuole. The Cvt complex that enters the vacuole, diffused throughout the vacuole in one minute (Figure 22). This result suggests that autophagic bodies disintegrate rapidly in the vacuole. Since the Cvt complex is localized to the pre-autophagosomal structure (Figure 19), it is plausible that the Cvt complex is formed on the pre-autophagosomal structure. Further studies of the dynamics of API-GFP will reveal the mechanism of the Cvt complex formation.

The factors involving the organization of the Cvt complex are still unknown. Cvt19p, a receptor for the Cvt transport (Scott *et al.*, 2001), was one candidate of such a factor, but the Cvt complex is formed normally in the Δ*cvt19* mutant (Figure 21), suggesting that other factors are involved in organizing the Cvt complex. Tlg2p and Vps45p, members of the Tlg1p t-SNARE complex, are specifically involved in the Cvt pathway, but not in autophagy (Abeliovich *et al.*, 1999). ProAPI accumulated in Δ*tlg2* and *vps45* mutants are membrane-bound but protease-accessible (Abeliovich *et al.*, 1999), indicating that these mutants have a defect in enwrapping proAPI into Cvt vesicles. Recently, Δ*vps45* mutant was shown to be completely blocked in API transport even under rapamycin-treated conditions (Hamasaki, personal communication). In addition, another group isolated a series of mutants named "*via* (vacuolar import and autophagocytosis" based on the absence of API enzymatic activity (Andrei-Selmer *et al.*, 2001). ProAPI in the *via* mutants does not form stable dodecamers and the enzymatic activity of API is not sufficiently restored by incubation in nitrogen starvation medium. By examining the localization of API-GFP in the above mutants, I will dissect the process of API transport to the vacuole.

In this study, I define a pre-autophagosomal structure, which is directly involved in the formation of autophagosomes. I also propose specific interrelationships between the many *APG* genes. Moreover, I constructed a strain expressing API-GFP, which is a useful marker to monitor the dynamics of Cvt vesicles and autophagosomes, and found that the Cvt complex accumulates on the pre-autophagosomal structure. Further study of the pre-autophagosomal structure will provide me with multiple insights into the precise understanding for the Cvt pathway and autophagy.

References

Abeliovich, H., Darsow, T. and Emr, S.D. (1999) Cytoplasm to vacuole trafficking of aminopeptidase I requires a t-SNARE-Sec1p complex composed of Tlg2p and Vps45p. *EMBO J.*, **18**, 6005-6016.

Abeliovich, H., Dunn, W.A., Jr, Kim, J. and Klionsky, D.J. (2000) Dissection of autophagosome biogenesis into distinct nucleation and expansion steps. *J. Cell Biol.*, **151**, 1025-1033.

Ahlberg, J. and Glaumann, H. (1985) Uptake-microautophagy-and degradation of exogenous proteins by isolated rat liver lysosomes. Effects of pH, ATP, and inhibitors of proteolysis. *Exp. Mol. Pathol.*, **42** 78-88.

Andrei-Selmer, C., Knuppel, A., Satyanarayana, C., Heese, C. and Schu, P.V. (2001) A new class of mutants deficient in dodecamerization of aminopeptidase 1 and vacuolar transport. *J. Biol. Chem.*, **276**, 11606-11614.

Aplin, A., Jasionowski, T., Tuttle, D.L., Lenk, S.E. and Dunn, W.A., Jr. (1992) Cytoskeletal elements are required for the formation and maturation of autophagic vacuoles. *J. Cell Physiol.*, **152**, 458-466.

Baba, M., Takeshige, K., Baba, N. and Ohsumi, Y. (1994) Ultrastructural analysis of the autophagic process in yeast: detection of autophagosomes and their characterization. *J. Cell Biol.*, **124**, 903-913.

Baba, M., Osumi, M. and Ohsumi, Y. (1995) Analysis of the membrane structures involved in autophagy in yeast by freeze-replica method. *Cell Struct. Funct.*, **20**, 465-472.

Baba, M., Osumi, M., Scott, S.V., Klionsky, D.J. and Ohsumi, Y. (1997) Two distinct pathways for targeting proteins from the cytoplasm to the vacuole/lysosome. *J. Cell Biol.*, **139**, 1687-1695.

Babst, M., Sato, T.K., Banta, L.M. and Emr, S.D. (1997) Endosomal transport function in yeast requires a novel AAA-type ATPase, Vps4p. *EMBO J.*, **16**, 1820-1831.

Blommaart, E.F., Krause, U., Schellens, J.P., Vreeling-Sindelarova, H. and Meijer, A.J. (1997) The phosphatidylinositol 3-kinase inhibitors wortmannin and LY294002 inhibit autophagy in isolated rat hepatocytes. *Eur. J. Biochem.*, **243**, 240-246.

Cadwell, R.C. and Joyce, G.F. (1995) Mutagenic PCR. In Dieffenbach, C. W. and Dveksler, G. S. (ed.), PCR PRIMER. Cold Spring Harbor Laboratory Press, Cold Spring Harbor, NY, U.S.A., pp. 583-589.

Chiang, H.L. and Schekman, R. (1991) Regulated import and degradation of a cytosolic protein in the yeast vacuole. *Nature*, **350**, 313-318.

Chiang, H.L., Schekman, R. and Hamamoto, S. (1996) Selective uptake of cytosolic, peroxisomal, and plasma membrane proteins into the yeast lysosome for degradation. *J. Biol. Chem.*, **271**, 9934-9941.

Ciechanover, A. (1998) The ubiquitin-proteasome pathway: on protein death and cell life. *EMBO J.*, **17**, 7151-7160.

Cuervo A.M. and Dice, J.F. (1996) A receptor for the selective uptake and degradation of proteins by lysosomes. *Science*, **273** 501-503.

Darsow, T., Rieder, S.E. and Emr, S.D. (1997) A multispecificity syntaxin homologue, Vam3p, essential for autophagic and biosynthetic protein transport to the vacuole. *J. Cell Biol.*, **138**, 517-529.

Davis, N.G., Horecka, J.L. and Sprague, G.F., Jr. (1993) Cis- and trans-acting functions required for endocytosis of the yeast phoromone receptors. *J. Cell Biol.*, **122**, 53-65.

Dice, J.F. (1990) Peptide sequences that target cytosolic proteins for lysosomal proteolysis. *Trends Biochem. Sci.*, **15**, 305-309.

Dunn, W.A., Jr. (1990a) Studies on the mechanisms of autophagy: maturation of the autophagic vacuole. *J. Cell Biol.*, **110**, 1935-1945.

Dunn, W.A., Jr. (1990b) Studies on the mechanisms of autophagy: formation of the autophagic vacuole. *J. Cell Biol.*, **110**, 1923-1933.

Dunn, W.A., Jr. (1994) Autophagy and related mechanisms of lysosome-mediated protein degradation. *Trends Cell Biol.*, **4**, 139-143.

Fengsrud, M., Roos, N., Berg, T., Liou, W., Slot, J.W. and Seglen, P.O. (1995) Ultrastructural and immunocytochemical characterization of autophagic vacuoles in isolated hepatocytes: effects of vinblastine and asparagine on vacuole distributions. *Exp. Cell Res.*, **221**, 504-519.

Fengsrud, M., Erichsen, E.S., Berg T.O., Raiborg, C. and Seglen, P.O. (2000) Ultrastructural characterization of the delimiting membranes of isolated autophagosomes and amphisomes by freeze-fracture electron microscopy. *Eur. J. Cell Biol.*, **79**, 871-882.

Funakoshi, T., Matsuura, A., Noda, T. and Ohsumi, Y. (1997). Analyses of APG13 gene involved in autophagy in yeast, *Saccharomyces cerevisiae*. *Gene*, **192**, 207-213.

Furukawa, K., Mizushima, N., Noda, T. and Ohsumi, Y. (2000) A protein conjugation system in yeast with homology to biosynthetic enzyme reaction of prokaryotes. *J. Biol. Chem.*, **275**, 7462-7465.

George, M.D., Baba, M., Scott, S.V., Mizushima, N., Garrison, B.S., Ohsumi, Y. and Klionsky, D.J. (2000) Apg5p functions in the sequestration step in the cytoplasm-to-vacuole targeting and macroautophagy pathways. *Mol. Biol. Cell*, **11**, 969-982.

Gordon, P.B., Kovacs, A.L. and Seglen, P.O. (1987) Temperature dependence of protein degradation, autophagic sequestration and mitochondrial sugar uptake in rat hepatocytes. *Biochim. Biophys. Acta.*, **929**, 128-133.

Harding, T.M., Hefner-Gravink, A., Thumm, M. and Klionsky, D.J. (1996) Genetic and phenotypic overlap between autophagy and the cytoplasm to vacuole protein targeting pathway. *J. Biol. Chem.*, **271**, 17621-17624.

Hershko, A. and Ciechanover, A. (1998) The ubiquitin system. *Annu. Rev. Biochem.*, **67**, 425-479.

Herskowitz, I. (1988) Life cycle of the budding yeast *Saccharomyces cerevisiae*. *Microbiol. Rev.*, **52**, 536-553.

Hicke, L. (2001) A new ticket for entry into budding vesicles – ubiquitin. *Cell*, **106**, 527-530.

Hochstrasser, M. (2000) Evolution and function of ubiquitin-like protein-conjugation systems. *Nat. Cell Biol.*, **2**, E153-E157.

Hilt, W. and Wolf, D.H. (1995) Proteasomes of the yeast *S. cerevisiae*: genes, structure and functions. *Mol. Biol. Rep.*, **21**, 3-10.

Hochstrasser, M. (1996) Ubiquitin-dependent protein degradation. *Annu. Rev. Genet.*, **30**, 405-439.

Hoffman, M. and Chiang, H.L. (1996) Isolation of degradation-deficient mutants defective in the targeting of fructose-1,6-bisphosphatase into the vacuole for degradation in *Saccharomyces cerevisiae*. *Genetics*, **143**, 1555-1566.

Holen, I., Gordon, P.B. and Seglen, P.O. (1993) Inhibition of hepatocytic autophagy by okadaic acid and other protein phosphatase inhibitors. *Eur. J. Biochem.*, **215**, 113-122.

Horvath, A. and Reizman, H. (1994) Rapid protein extraction from *Saccharomyces cerevisiae*. *Yeast*, **10**, 1304-1310.

Huang, P.H. and Chiang, H.L. (1997) Identification of novel vesicles in the cytosol to vacuole protein degradation pathway. *J. Cell Biol.*, **136**, 803-810.

Huang, W.P., Scott, S. V., Kim, J. and Klionsky, D.J. (2000) The itinerary of a vesicle component, Aut7p/Cvt5p, terminates in the yeast vacuole via the autophagy/Cvt pathways. *J. Biol. Chem.*, **275**, 5845-5851.

Ichimura, Y., Kirisako, T., Takao, T., Satomi, Y., Shimonishi, Y., Ishihara, N., Mizushima, N., Tanida, I., Kominami, E., Ohsumi, M., Noda, T. and Ohsumi, Y. (2000) A ubiquitin-like system mediates protein lipidation. *Nature*, **408**, 488-492.

Johnson, E.S., Schwienhorst, I. Dohmen, R.J. and Blobel, G. (1997) The ubiquitin-like protein Smt3p is activated for conjugation to other proteins by an Aos1p/Uba2p heterodimer. *EMBO J.*, **16**, 5509-5519.

Jones, E.W. (1984) The synthesis and function of proteases in *Saccharomyces*: genetic approaches. *Annu. Rev. Genet.*, **18**, 233-270.

Kabeya, Y., Mizushima, N., Ueno, T., Yamamoto, A., Kirisako, T., Noda, T., Kominami, E., Ohsumi, Y. and Yoshimori, T. (2000) LC3, a mammalian homologue of yeast Apg8p, is localized in autophagosome membranes after processing. *EMBO J.*, **19**, 5720-5728.

Kaiser, C., Michaelis, S. and Mitchell, A. (1994) Methods in Yeast Genetics. Cold Spring Harbor Laboratory Press, Cold Spring Harbor, NY.

Kamada, Y., Funakoshi, T., Shintani, T., Nagano, K., Ohsumi, M. and Ohsumi, Y. (2000) Tor-mediated induction of autophagy via an Apg1 protein kinase complex. *J. Cell Biol.*, **150**, 1507-1513.

Kametaka, S., Matsuura, A., Wada, Y. and Ohsumi, Y. (1996) Structural and functional analyses of APG5, a gene involved in autophagy in yeast. *Gene*, **178**, 139-143.

Kametaka, S., Okano, T., Ohsumi, M. and Ohsumi, Y. (1998) Apg14p and Apg6/Vps30p form a protein complex essential for autophagy in the yeast, *Saccharomyces cerevisiae*. *J. Biol. Chem.*, **273**, 22284-22291.

Kaneko, Y., Toh-e, A. and Oshima, Y. (1982) Identification of the genetic locus for the structural gene and a new regulatory gene for the synthesis of repressible alkaline phosphatase in *Saccharomyces cerevisiae*. *Mol. Cell Biol.*, **2**, 127-137.

Kihara, A., Noda, T., Ishihara, N. and Ohsumi, Y. (2001a) Two distinct Vps34 PtdIns 3-kinase complexes function in autophagy and CPY sorting in *Saccharomyces cerevisiae*. *J. Cell Biol.*, **152**, 519-530.

Kihara, A., Kabeya, Y., Ohsumi, Y. and Yoshimori, T. (2001b) Beclin-phosphatidylinositol 3-kinase complex functions at the *trans*-Golgi network. *EMBO Rep.*, **2**, 330-335.

Kim, J., Scott, S.V., Oda, M. and Klionsky, D.J. (1997) Transport of a large oligomeric protein by the cytoplasm to vacuole protein targeting pathway. *J. Cell Biol.*, **137**, 609-618.

Kim, J., Dalton, V.M., Eggerton, K.P., Scott. S.V. and Klionsky, D.J. (1999) Apg7p/Cvt2p is required for the cytoplasm-to-vacuole targeting, macroautophagy, and peroxisome degradation pathways. *Mol. Biol. Cell*, **10**, 1337-1351.

Kim, J. and Klionsky, D.J. (2000) Autophagy, cytoplasm-to-vacuole targeting pathway, and pexophagy in yeast and mammalian cells. *Annu. Rev. Biochem.*, **69**, 303-342.

Kim, J., Huang, W.P. and Klionsky, D.J. (2001) Membrane recruitment of Aut7p in the autophagy and cytoplasm to vacuole targeting pathways requires Aut1p, Aut2p, and the autophagy conjugation complex. *J. Cell. Biol.*, **152**, 51-64.

Kirisako, T., Baba, M., Ishihara, N., Miyazawa, K., Ohsumi, M., Yoshimori, T., Noda, T. and Ohsumi, Y. (1999) Formation process of autophagosome is traced with Apg8/Aut7p in yeast. *J. Cell Biol.*, **147**, 435-446.

Kirisako, T., Ichimura, Y., Okada, H., Kabeya, Y., Mizushima, N., Yoshimori, T., Ohsumi, M., Takao, T., Noda, T. and Ohsumi, Y. (2000) The reversible modification regulates the membrane-binding state of Apg8/Aut7 essential for autophagy and the cytoplasm to vacuole targeting pathway. *J. Cell Biol.*, **151**, 263-276.

Klionsky, D.J., Herman, P.K. and Emr, S.D. (1990) The fungal vacuole: composition, function, and biogenesis. *Microbiol. Rev.*, **54**, 266-292.

Klionsky, D.J., Cueva, R. and Yaver, D.S. (1992) Aminopeptidase I of *Saccharomyces cerevisiae* is localized to the vacuole independent of the secretory pathway. *J. Cell Biol.*, **119**, 287-299.

Kornfeld, S. and Mellman, I. (1989) The biogenesis of lysosomes. *Annu. Rev. Cell Biol.*, **5**, 483-525.

Kornfeld, S. (1992) Structure and function of the mannose 6-phosphate/insulinlike growth factor II receptors. *Annu. Rev. Biochem.*, **61**, 307-330.

Kovacs, A.L., Reith, A. and Seglen, P.O. (1982) Accumulation of autophagosomes after inhibition of hepatocytic protein degradation by vinblastine, leupeptin or a lysosomotropic amine. *Exp. Cell Res.*, **137**, 191-201.

Lammer, D., Mathias, N., Laplaza, J.M., Jiang, W., Liu, Y., Callis, J., Goebl, M. and Estelle, M. (1998) Modification of yeast Cdc53p by the ubiquitin-related protein rub1p affects function of the SCFSdc4 complex. *Genes Dev.*, **12**, 914-926.

Lenk, S.E., Fisher, D.L. and Dunn, W.A., Jr. (1991) Regulation of protein secretion by crinophagy in perfused rat liver. *Eur. J. Cell Biol.*, **56**, 201-209.

Liakopoulos, D., Doenges, G., Matuschewski, K. and Jentsch, S. (1998) A novel protein modification pathway related to the ubiquitin system. *EMBO J.*, **17**, 2208-2214.

Liang, X.H., Jackson, S., Seaman, M., Brown, K., Kempkes, B., Hibshoosh, H. and Levine, B. (1999) Induction of autophagy and inhibition of tumorigenesis by *beclin 1*. *Nature*, **402**, 672-676.

Lillie, S.H. and Pringle, J.R. (1980) Reserve carbohydrate metabolism in *Saccharomyces cerevisiae*: responses to nutrient limitation. *J. Bacteriol.*, **143**, 1384-1394.

Loeb, K.R. and Haas, A.L. (1992) The interferon-inducible 15-kDa ubiquitin homolog conjugates to intracellular proteins. *J. Biol. Chem.*, **267**, 7806-7813.

Longtine, M.S., Mckenzie III, A., Demarini, D.J., Shar, N.G., Wach, A., Brachat, A., Philippsen, P. and Pringle, J.R. (1998) Additional modules for versatile and economical PCR-based gene deletion and modification in *Saccharomyces cerevisiae*. *Yeast*, **14**, 953-961.

Luo, W. and Chang, A. (1997) Novel genes involved in endosomal traffic in yeast revealed by suppression of a targeting-defective plasma membrane ATPase mutant. *J. Cell Biol.*, **138**, 731-746.

Mahajan, R., Delphin, C., Guan, T., Gerace, L. and Melchior, F. (1997) A small ubiquitin-related polypeptide involved in targeting RanGAP1 to nuclear pore complex protein RanBP2. *Cell*, **88**, 97-107.

Matsuura, A., Tsukada, M., Wada, Y. and Ohsumi, Y. (1997) Apg1p, a novel protein kinase required for the autophagic process in *Saccharomyces cerevisiae*. *Gene*, **192**, 245-250.

Matunis, M.J., Coutavas, E. and Blobel, G. (1996) A novel ubiquitin-like modification modulates the partitioning of the Ran-GTPase-activating protein RanGAP1 between the cytosol and the nuclear pore complex. *J. Cell Biol.*, **135**, 1457-1470.

Mizushima, N., Noda, T., Yoshimori, T., Tanaka, Y., Ishii, T., George, M.D., Klionsky, D.J., Ohsumi, M. and Ohsumi, Y. (1998) A protein conjugation system essential for autophagy. *Nature*, **395**, 395-398.

Mizushima, N., Noda, T. and Ohsumi, Y. (1999) Apg16p is required for the function of the Apg12p-Apg5p conjugate in the yeast autophagy pathway. *EMBO J.*, **18**, 3888-3896.

Mizushima, N., Yamamoto, A., Hatano, M., Kobayashi, Y., Kabeya, Y., Suzuki, K., Tokuhisa, T., Ohsumi, Y. and Yoshimori, T. (2001) Dissection of autophagosome formation using Apg5-deficient mouse embryonic stem cells. *J. Cell Biol.*, **152**, 657-667.

Mortimore, G.E., Lardeux, B.R. and Adams, C.E. (1988) Regulation of microautophagy and basal protein turnover in rat liver. Effects of short-term starvation. *J. Biol. Chem.*, **263**, 2506-2512.

Mortimore, G.E., Poso, A.R. and Lardeux, B.R. (1989) Mechanism and regulation of protein degradation in liver [published erratum appears in *Diabetes Metab. Rev.*, 1989, **5**, 320]. *Diabetes Metab. Rev.*, **5**, 338-344.

Mortimore, G.E., Miotto, G., Venerando, R. and Kadowaki, M. (1996) Autophagy, *Subcell. Biochem.*, **27**, 93-135.

Nishikawa, S., Hirata, A. and Nakano, A. (1994) Inhibition of endoplasmic reticulum (ER)-to-Golgi transport induces relocalization of binding protein (BiP) within the ER to form the BiP bodies. *Mol. Biol. Cell*, **5**, 1129-1143.

Noda, T., Matsuura, A., Wada, Y. and Ohsumi, Y. (1995) Novel system for monitoring autophagy in the yeast *Saccharomyces cerevisiae*. *Biochem. Biophys. Res. Commun.* **210**, 126-132.

Noda, T. and Ohsumi, Y. (1998) Tor, a phosphatidylinositol kinase homologue, controls autophagy in yeast. *J. Biol. Chem.*, **273**, 3963-3966.

Noda, T., Kim, J., Huang, W.P., Baba, M., Tokunaga, C., Ohsumi, Y. and Klionsky, D.J. (2000) Apg9p/Cvt7p is an integral membrane protein required for transport vesicle formation in the Cvt and autophagy pathways. *J. Cell Biol.*, **148**, 465-480.

Osaka, F., Kawasaki, H., Aida, N., Saeki, M., Chiba, T., Kawashima, S., Tanaka, K. and Kato, S. (1998) A new NEDD8-ligating system for cullin-4A. *Genes Dev.*, **12**, 2263-2268.

Petiot, A., Ogier-Denis, E., Blommaart, E.F., Meijer, A.J. and Codogno, P. (2000) Distinct classes of phosphatidylinositol 3'-kinases are involved in signaling pathways that control macroautophagy in HT-29 cells. *J. Biol. Chem.*, **275**, 992-998.

Piper, R.C., Cooper, A.A., Yang, H. and Stevens, T.H. (1995) *VPS27* controls vacuolar and endocytic traffic through a prevacuolar compartment in *Saccharomyces cerevisiae*. *J. Cell Biol.*, **131**, 603-617.

Plomp, P.J., Wolvetang, E.J., Groen, A.K., Meijer, A.J., Gordon, P.B. and Seglen, P.O. (1987) Energy dependence of autophagic protein degradation in isolated rat hepatocytes. *Eur. J. Biochem.*, **164**, 197-203.

Raymond, C.K., Howald-Stevenson, I., Vater, C.A. and Stevens, T.H. (1992) Morphological classification of the yeast vacuolar protein sorting mutants: evidence for a prevacuolar compartment in class E *vps* mutants. *Mol. Biol. Cell*, **3**, 1389-1402.

Rieder, S.E., Banta, L.M., McCaffery, J.M. and Emr, S.D. (1996) Multilamellar endosome-like compartment accumulates in the yeast *vps28* vacuolar protein sorting mutant. *Mol. Biol. Cell*, **7**, 985-999.

Schworer, C.M., Shiffer, K.A. and Mortimore, G.E. (1981) Quantitative relationship between autophagy and proteolysis during graded amino acid deprivation in perfused rat liver. *J. Biol. Chem.*, **256**, 7652-7658.

Scott, S.V., Baba, M., Ohsumi, Y. and Klionsky, D.J. (1997) Aminopeptidase I is targeted to the vacuole by a nonclassical vesicular mechanism. *J. Cell Biol.*, **138**, 37-44.

Scott, S.V., Guan, J., Hutchins, M.U., Kim, J. and Klionsky, D.J. (2001) Cvt19 is a receptor for the cytoplasm-to-vacuole targeting pathway. *Mol. Cell*, **7**, 1131-1141.

Seglen, P.O. (1987) Regulation of autophagic protein degradation in isolated liver cells. In Glaumann, H. and Ballard, F.J. (ed.), Lysosomes: Their Role in Protein Breakdown. Academic Press, London, UK., pp. 371-414.

Seglen, P.O. and Gordon, P.B. (1982) 3-Methyladenine: specific inhibitor of autophagic/lysosomal protein degradation in isolated rat hepatocytes. *Proc. Natl. Acad. Sci. U.S.A.*, **79**, 1889-1892.

Seglen, P.O. and Bohley, P. (1992) Autophagy and other vacuolar protein degradation mechanisms. *Experientia*, **48**, 158-172.

Segui-Real, B., Martinez, M. and Sandoval, I.V. (1995) Yeast aminopeptidase I is post-translationally sorted from the cytosol to the vacuole by a mechanism mediated by its bipartite N-terminal extension. *EMBO J.*, **14**, 5476-5484.

Shintani, T., Mizushima, N., Ogawa, Y., Matsuura, A., Noda, T. and Ohsumi, Y. (1999) Apg10p, a novel protein-conjugating enzyme essential for autophagy in yeast. *EMBO J.*, **18**, 5234-5241.

Shintani, T., Suzuki, K., Kamada, Y., Noda, T. and Ohsumi, Y. (2001) Apg2p functions in autophagosome formation on the perivacuolar structure. *J. Biol. Chem.*, **276**, 30452-30460.

Shirahama, K., Noda, T. and Ohsumi, Y. (1997) Mutational analysis of Csc1/Vps4p: involvement of endosome in the regulation of autophagy in yeast. *Cell Struct. Funct.*, **22**, 501-509.

Shieh, H.L., Chen, Y., Brown, C.R. and Chiang, H.L. (2001) Biochemical analysis of fructose-1,6-bisphosphatase import into vacuole import and degradation vesicles reveals a role for *UBC1* in vesicle biogenesis. *J. Biol. Chem.*, **276**, 10398-10406.

Takeshige, K., Baba, M., Tsuboi, S., Noda, T. and Ohsumi, Y. (1992) Autophagy in yeast demonstrated with proteinase-deficient mutants and conditions for its induction. *J. Cell Biol.*, **119**, 301-311.

Tanida, I., Mizushima, N., Kiyooka, M., Ohsumi, M., Ueno, T., Ohsumi, Y. and Kominami, E. (1999) Apg7p/Cvt2p: A novel protein-activating enzyme essential for autophagy. *Mol. Biol. Cell*, **10**, 1367-1379.

Teichert, U., Mechler, B., Muller, H. and Wolf, D.H. (1989) Lysosomal (vacuolar) proteinases of yeast are essential catalysts for protein degradation, differentiation, and cell survival. *J. Biol. Chem.*, **264**, 16037-16045.

Terlecky, S.R., Chiang, H-L., Olson, T.S. and Dice, J.F. (1992) Protein and peptide binding and stimulation of in vitro lysosomal proteolysis by the 73-kDa heat shock cognate protein. *J. Biol. Chem.*, **267**, 9202-9209.

Thumm, M., Egner, R., Koch, M., Schlumpberger, M., Straub, M., *et al.* (1994) Isolation of autophagocytosis mutants of *Saccharomyces cerevisiae*. *FEBS Lett.*, **349**, 275-280.

Tsukada, M. and Ohsumi, Y. (1993) Isolation and characterization of autophagy-defective mutants of *Saccharomyces cerevisiae*. *FEBS Lett.*, **333**, 169-174

Tuttle, D.L. and Dunn, W.A., Jr. (1995) Divergent modes of autophagy in the methylotrophic yeast *Pichia pastoris*. *J. Cell Sci.*, **108**, 25-35.

Ueno, T., Muno, D. and Kominami, E. (1991) Membrane markers of endoplasmic reticulum preserved in autophagic vacuolar membranes isolated from leupeptin-administered rat liver. *J. Biol. Chem.*, **266**, 18995-18999.

Varshavsky, A. (1997) The ubiquitin system. *Trends Biochem. Sci.*, **22**, 383-387.

Vida, T.A., Huyer, G. and Emr, S.D. (1993) Yeast vacuolar proenzymes are sorted in the late Golgi complex and transported to the vacuole via a prevacuolar endosome-like compartment. *J. Cell Biol.*, **121**, 1245-1256.

Vida, T.A. and Emr, S.D. (1995) A new vital stain for visualizing vacuolar membrane dynamics and endocytosis in yeast. *J. Cell Biol.*, **128**, 779-792.

Yamamoto, A., Masaki, R. and Tashiro, Y. (1990) Characterization of the isolation membranes and the limiting membranes of autophagosomes in rat hepatocytes by lectin cytochemistry. *J. Histochem. Cytochem.*, **38**, 573-580.

Yoshihisa, T. and Anraku, Y. (1990) A novel pathway of import of α-mannosidase, a marker enzyme of vacuolar membranes in *Saccharomyces cerevisiae*. *J. Biol. Chem.*, **263**, 5158-5163.

Yuan, W.Y., Tuttle, D.L., Shi, Y-J., Ralph, G.S. and Dunn, W.A., Jr. (1997) Glucose-induced microautophagy in *Pichia pastoris* requires the α-subunit of phosphofructokinase. *J. Cell Sci.*, **110**, 1935-1945.

Yuan, W., Strømhaug, P.E. and Dunn, W.A., Jr (1999) Glucose-induced autophagy of peroxisomes in *Pichia pastoris* requires a unique E1-like protein. *Mol. Biol. Cell*, **10**, 1353-1366

Zubenko, G.S. and Jones, E.W. (1981) Protein degradation, meiosis and sporulation in proteinase-deficient mutants of *Saccharomyces cerevisiae*. *Genetics*, **97**, 45-64.